R-13-48

Chemical and mineralogical characterization of the Indian tunnel backfill bentonite Asha NW BFL-L 2010

Siv Olsson, Ola Karnland
Clay Technology AB

Daniel Svensson, Christel Lundgren
Svensk Kärnbränslehantering AB

December 2013

Svensk Kärnbränslehantering AB
Swedish Nuclear Fuel
and Waste Management Co

Box 250, SE-101 24 Stockholm
Phone +46 8 459 84 00

ISSN 1402-3091
SKB R-13-48
ID 1396086

Chemical and mineralogical characterization of the Indian tunnel backfill bentonite Asha NW BFL-L 2010

Siv Olsson, Ola Karnland
Clay Technology AB

Daniel Svensson, Christel Lundgren
Svensk Kärnbränslehantering AB

December 2013

Abstract

An Indian bentonite candidate for tunnel backfill, Asha NW BFL-L 2010 (in this report abbreviated ABF) was analysed using selected methods for a chemical and mineralogical characterization in order to evaluate its conformity to the reference backfill material, which is a bentonite clay with a nominal montmorillonite content of 50–60 weight percent and an accepted variation within 45–90 wt% (SKB 2010). Several of the material parameters relevant in the quality assessment of bentonites were determined in parallel at Clay Technology AB, Lund, and at SKB's laboratory at Äspö as part of SKB's competence build up program (SKB project KBP 4002-11-1: Kunskapsöverföring). The results obtained at Clay Technology AB are presented in the first part of this report and the results obtained by SKB at the Äspö laboratory in the second part.

As received the bentonite was an inhomogeneous material. This could be seen visually, such as large variations in the grain-size distribution and colour of the laboratory samples, as well as experimentally. As for all inhomogeneous materials, one of the most difficult aspects of establishing a specific material parameter is to obtain a small, representative sample for laboratory tests. In order to assess uncertainties related to material inhomogeneity, separate analyses were performed of aggregates >2 mm sorted by colour and of particles <1 mm from some randomly selected laboratory samples. In general, the coarse aggregates had higher smectite proportion than the fine-grained matrix of the bentonite and the overall mineralogy differed with respect to abundance and type of accessory minerals. Hence sampling errors potentially exist yielding samples of poor representativeness if particles are segregated by size during handling and sampling of the 1250 kg sacks with bentonite. In order to reduce these errors a sampling plan designed for inhomogeneous materials should be applied.

The total sulphur content of the bentonite samples from the ABF 2010 batch was close to or below the detection limit (0.02% S) of the analytical method and the major source of sulphur was sulphates. The total carbon content of the samples ranged from 0.41 to 0.95% C, and the predominant carbon source was calcite, although the carbon data for the purified <0.5 μm fractions suggested that minor amounts of colloidal organic matter may exist.

According to the producer, Ashapura Minechem Co., the bentonite ABF 2010 has a montmorillonite content of 69%. Mineral quantification by use of the Siroquant software gave an average smectite content in the ABF samples (excl. sorted samples) of 74% and the range of variation was 69 to 79%. Judged by the X-ray diffraction characteristics, the swelling clay mineral is a dioctahedral smectite of the montmorillonite–beidellite series, but the available XRD-data are inadequate for distinguishing the members of the series at a species-level. The structural formulae calculated on the chemistry of purified <0.5 μm fractions suggested that more than 50% of the charge is located in the tetrahedral sheet and, according to international nomenclature recommendations, the smectite should be classified as beidellite rather than montmorillonite. However, remnant impurities (kaolin, iron oxides) in the <0.5 μm fractions may result in overestimation of the tetrahedral charge, and the identification of the members in the montmorillonite–beidellite series at a species level should be verified by independent tests to determine the charge distribution. The bentonite samples also include a 7 Å-phase interpreted as a kaolin mineral, which was confirmed by scans of heated samples – kaolin minerals, in contrast to chlorites, become amorphous upon heating.

Sammanfattning

En indisk bentonit, Asha NW BFL-L, 2010 (i denna rapport förkortad ABF) analyserades med hjälp av några utvalda standardmetoder för kemisk och mineralogisk karaktärisering i syfte att utvärdera dess överensstämmelse med specifikationerna för ett återfyllningsmaterial. Nuvarande referens för återfyllnadsmaterial är bentonitlera med en nominell montmorillonithalt på 50–60 viktprocent och en tillåten variation inom 45–90 vikt% (SKB 2010). Flera materialparametrar som är relevanta i kvalitetsbedömning av bentonit bestämdes parallellt på Clay Technology AB, Lund, och vid SKB:s laboratorium på Äspö som en del av SKB:s kompetensuppbyggnadsprogram (SKB projekt KBP 4002-11-1; Kunskapsöverföring). De resultat som erhållits vid Clay Technology AB presenteras i den första delen av denna rapport och de resultat som uppnåtts vid Äspölaboratoriet i den andra delen.

Bentoniten var inhomogen, vilket kunde ses visuellt, t.ex. som variationer i kornstorlek och färg på laboratorieproverna, samt experimentellt. En av svårigheterna vid provtagning av inhomogena material är att få fram ett tillräckligt litet men ändå representativt prov för analys. För att bedöma osäkerheter relaterade till materialinhomogenitet gjordes separata analyser på aggregat > 2 mm, sorterade efter färg, och av partiklar <1 mm från några slumpvis utvalda laboratorieprover. I allmänhet hade de grövre aggregaten högre smektithalt än de finkorniga och mineralogin skilde med avseende på mängd och typ av accessoriska mineral. Det finns således en risk att representativiteten hos laboratorieproven blir dålig om partiklar sorterats efter storlek under hantering och provtagning av de 1250 kg säckar bentoniten levererades i. För att minska denna risk bör en provtagningsplan avsedd för inhomogena material tillämpas.

Den totala svavelhalten i bentoniten var nära eller under detektionsgränsen (0,02 % S) för analysmetoden (Leco) och den största svavelkällan var sulfater. Den totala kolhalten i proverna varierade från 0,41 till 0,95 % C, och den dominerande kolkällan var kalcit, även om koldata för renade <0,5 µm fraktioner indikerade att mindre mängder av kolloidalt organiskt material kan finnas.

Enligt leverantören, Ashapura Minechem Co, har bentoniten ABF 2010 en montmorillonithalt på 69 %. Mineralkvantifiering gjord med programvaran Siroquant enligt standardrutiner gav ett genomsnittligt smektitinnehåll i ABF proverna (exkl. sorterade prover) på 74 %, med en variation mellan 69 och 79 %. Enligt röntgendiffraktionsdata är det svällande lermineralet en dioktaedrisk smektit tillhörande montmorillonit-beidellit serien, men tillgängliga data är otillräckliga för att identifiera smektiten på detaljnivå. Strukturformler beräknade på kemin av renade <0,5 µm fraktioner tydde på att mer än 50 % av laddningen finns i tetraederskiktet och enligt internationell nomenklatur bör en sådan smektit klassificeras som beidellit snarare än montmorillonit. Dock kan föroreningar i form av kaolin och järnoxid i <0,5 µm fraktionerna resultera i att tetraederladdningen överskattas, varför en oberoende metod för bestämning av laddningsfördelningen rekommenderas. Proven innehöll även en 7 Å-fas som tolkats som ett kaolin mineral, vilket bekräftades genom röntgen av upphettade prov.

Contents

1 Introduction

An Indian candidate backfill bentonite, Asha NW BFL-L 2010, (abbreviated ABF in this report) was analysed by use of some selected "standard" methods for a chemical and mineralogical characterization in order to evaluate its conformity to the reference backfill material, which is bentonite clay with a nominal montmorillonite content of 50–60 weight % and an accepted variation within 45–90% (SKB 2010). According to the producer, Ashapura Minechem Co., the bentonite Asha NW BFL-L 2010 has a montmorillonite content of 69%.

Several of the material parameters relevant in the quality assessment of bentonites were determined in parallel at Clay Technology AB, Lund, and at SKB's laboratory at Äspö as part of SKB's competence build up program (SKB project KBP 4002-11-1: Kunskapsöverföring). The results obtained at Clay Technology AB are presented in the first part of this report and the results obtained at the Äspö laboratory in the second part.

The original scope of the project was:

(1) Bulk chemical analysis of the bentonite.

(2) Mineralogical content using X-ray diffraction (XRD).

(3) Cation exchange capacity (CEC) using the copper triethylenetetramine method.

(4) Exchangeable cation extraction (EC).

(5) Mineral grain density.

(6) Surface area determination using BET.

(7) Grain size distribution.

(8) Water content.

(9) Chemical analysis of the clay fraction after dialysis.

(10) Cation exchange capacity of the clay fraction.

(11) Free swelling.

The project had strict time and cost limitations, hence all tests were not performed. However, the activities were transferred to another SKB project (KBP1009) for further material knowledge and competence development.

2 Material and methods

2.1 Test matrix

The bentonite was delivered in 2010 from Ashapura Minechem Co. in 1250 kg sacks, which were sampled at the Äspö laboratory and delivered to Clay Technology AB in 250 ml polyethene bottles. Seven of the laboratory samples, labelled with the number of the bottles/sacks (Table 2-1) and with weights ranging from 170 to 230 g, were homogenized by grinding the entire sample in a ball mill after drying at 60ºC. One of the ground samples, ABF 70, was divided into five subsamples for repeatability tests.

During the grinding it was noticed that the hardness, colour, and proportion of gravel-sized bentonite aggregates (>2 mm) varied significantly among the samples (Figure 2-1). In general, the colour of the hardest aggregates differed from that of the matrix of the bentonite, and, as a consequence, the colour of the ground bentonite powders varied from reddish to yellowish-brown, depending on the type and abundance of aggregates in the starting material. In order to assess uncertainties related to material inhomogeneity caused by a possible particle-size segregation during handling and sampling of the 1250 kg sacks, grains with a size >2 mm were separated by dry-sieving of three randomly selected samples (ABF 5, 80 and 90) and sorted by colour into four fractions (grey, red, green, brown) before grinding. The remnant material was sieved at a mesh-size of 1 mm, and the <1 mm fraction was ground and treated as a separate sample (Figure 2-1). The absolute proportions of the coloured grains in the three samples could not be determined but the abundance in the >2 mm fractions was Brown>Green≈Grey>Red. The grain-size distribution determined by dry-sieving two Asha samples (Figure 2-2; from Sandén et al. 2013) in the "as-received state" suggests that aggregates >2 mm may represent 40–60% of the material. The test matrix is compiled in Table 2-1. In the following text the term "bulk material" includes the samples that were sorted prior to grinding, unless otherwise stated.

Table 2-1. Test matrix. ABF=Asha NW BFL-L 2010, number=number of sack; other suffixes in the labels are explained in the text.

Sample id	Bulk*					<0.5 µm fraction				Notes
	WS	XRD	CEC	EC	Chemical comp	XRD AD	XRD EG	CEC	Chemical comp	
ABF 10	1	1	2	1	1	1	1	2	1	reddish
ABF 15	1	1	2	1	1	1	1	2	1	
ABF 40	1	1	2	1	1	1	1	2	1	
ABF 55	1	1	2	1	1	1	1	2	1	yellowish;fine-grained
ABF 60	1	1	2	1	1	1	1	2	1	
ABF 70	3	5	3×2	5	5	3	3	3×2	5	
ABF 100	1	1	2	1	1	1	1	2	1	reddish
ABF Red	1	1	2	1	1	1	1	2	1	>2 mm of 5+80+90
ABF Grey	1	1	2	1	1	1	1	2	1	”
ABF Green	1	1	2	1	1	1	1	2	1	”
ABF Brown	1	1	2	1	1	1	1	2	1	”
ABF <1 mm	1	1	2	1	1	1	1	2	1	<1 mm of 5+80+90 yellowish

* "bulk" includes the sorted samples; WS=water-soluble salts; XRD = X-ray diffraction; CEC = cation exchange capacity; EC=exchangeable cations; AD=air-dried; EG=ethylene glycol solvated.

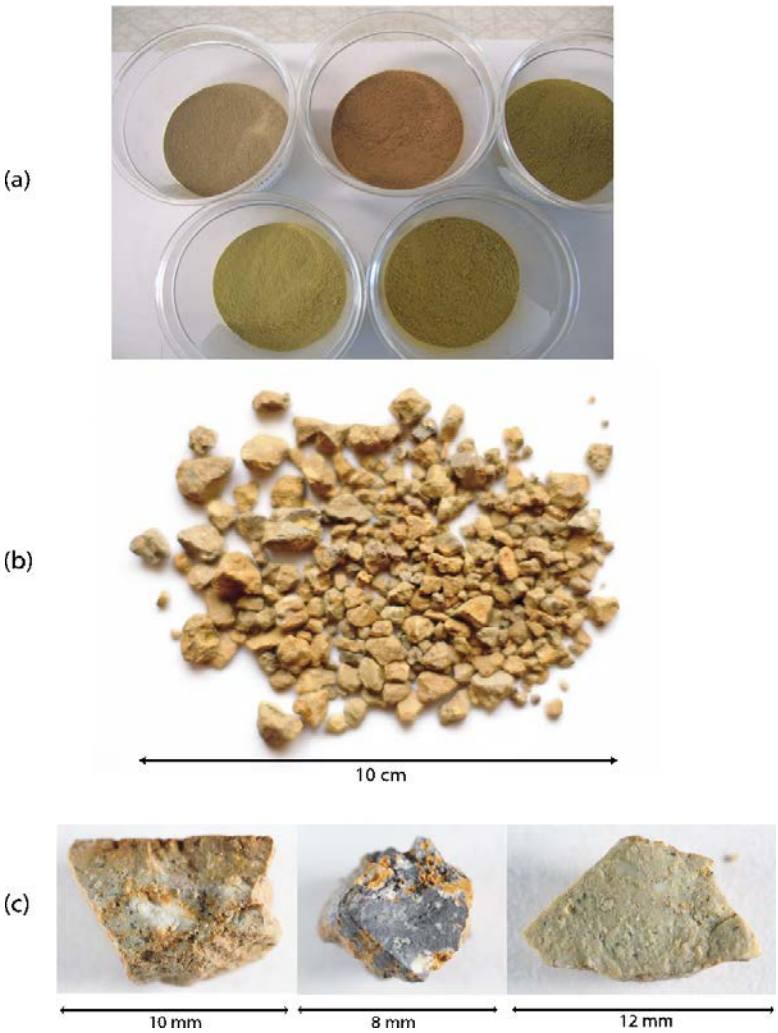

Figure 2-1. *(a) Powders of the gravel-sized bentonite aggregates that were sorted by colour before grinding. The samples in the upper row were labelled Grey, Red, <1 mm and samples in the lower row Green and Brown (from left to right). (b) sample ABF 10 in the as-received state. (c) large aggregates with fresh surfaces from sample ABF 10.*

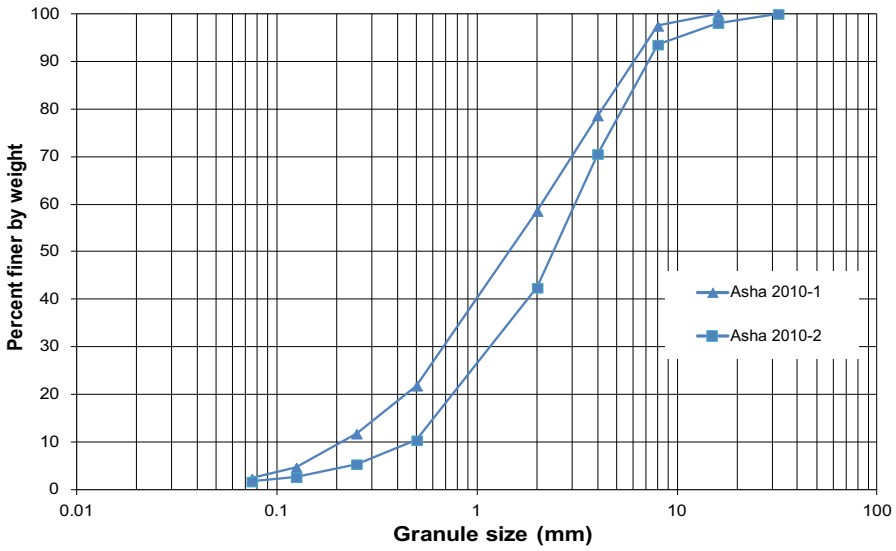

Figure 2-2. *Granule-size distribution of two Asha bentonite samples in the "as-received state". From Sandén et al. (2013).*

2.2 Sample pre-treatment

Both the bulk material and the Na-converted <0.5 µm fractions of the samples were analysed for mineralogy, cation exchange capacity, and chemical composition.

In order to get as pure a smectite fraction as possible, thereby making element allocations in formula calculations less ambiguous, the <0.5 µm fraction, instead of the conventional <2 µm clay fraction, was chosen. Furthermore, the clay was saturated with one single, non-structural cation – in this case sodium– to make the allocation of cations in formula calculations to exchange and structural sites, respectively, less ambiguous.

In order to facilitate separation of the <0.5 µm fraction, the bentonite was first suspended in deionised water and the clay was converted to homo-ionic Na-clay by addition of NaCl p.a. (final concentration 1M), followed by centrifugation and decantation of the clear supernatant.

The procedure was repeated twice. Excess salt was thereafter removed by repeated washings, which were followed by dialysis (Spectrapore 3. 3500 MWCO dialysis membrane) against deionized water until the electrical conductivity of the external water remained <10 µS/cm for five days. After completed dialysis the slurry was dispersed in deionized water and centrifuged with a centrifugation time/speed calculated by use of Stokes´ Law to correspond to a particle separation at an equivalent diameter of 0.5 µm. After separation, the fine clay fraction was again treated with NaCl and dialyzed, and, finally, dried at 60°C and ground.

2.3 Aqueous leachates

Aqueous leaching of the bulk samples was used to obtain information about the composition of solutes and soluble salts in the bentonite. The dried (105ºC) and ground bentonite was dispersed in deionised water (solid:liquid ratio 1:100) by ultrasonic treatment for 30 minutes and stirring overnight. The suspension was left for 5 days at room temperature to allow equilibration and sedimentation. After phase separation by centrifugation and stepwise ultra-filtration using filters of decreasing pore size (from 2 to 0.2 µm syringe filters Acrodisc PF), major anions and inorganic C were determined by use of ion chromatography and a C/N analyser, respectively, at the Department of Biology, Lund University. The electrical conductivity of the leachates was determined by use of a Metrohm conductometer.

2.4 Cation exchange capacity (CEC) and exchangeable cations

The cation exchange capacity (CEC) of bulk materials and of fractions <0.5 µm was determined by exchange with copper(II)triethylenetetramine following the procedure of Meier and Kahr (1999), modified according to Ammann et al. (2005). The reagent solution was prepared of anhydrous $CuSO_4$, dried at 250°C before use. Sample mass and Cu-trien concentration were matched to ascertain that the maximum adsorption of the index cation should not exceed ~60%, to assure a high level of cation exchange.

The ground sample (~0.4 g) was fully dispersed in 50 ml deionised water by ultrasonic treatment and shaking. 20 ml of ~20 mM Cu(II)-triethylenetetramine solution was added to the suspension, which was left to react for 30 minutes on a vibrating table. After centrifugation, the absorbance at 620 nm of the supernatant was measured using a spectrophotometer (Shimadzu) and CEC calculated on the basis of the uptake of Cu by the clay. The water content of the bulk samples was determined for a separate sample dried at 105ºC for 24 h. Due to lack of material, the latter step in the procedure was omitted for the Na-converted <0.5 µm fractions, which instead were dried at 105ºC prior to analysis. All CEC determinations were duplicated.

Soluble minerals like gypsum and calcite will dissolve in the aqueous Cu-trien solution, which makes this extractant unsuitable for determining the exchangeable cations. Therefore, the exchangeable cations were extracted by three successive displacements with ammonium in an alcoholic solution (0.15 M NH_4Cl in ~80% ethanol) according to a procedure originally recommended for CEC determinations of gypsiferous/calcareous soils (e.g. Belyayeva 1967). An alcoholic solution certainly minimizes dissolution of gypsum and calcite, but chlorides, sulphates and carbonates of alkali metals, if present, will dissolve also in this extractant.

0.8 g of the ground sample was shaken for 30 minutes in approximately one third of a total volume of 50 ml of the extractant. After centrifugation the supernatant was collected. This treatment was repeated three times. After evaporation of the alcohol and adjustment of the volume with deionised water, the concentration of Ca, Mg, Na, and K was determined by use of ICP-AES at the Department of Biology, Lund University. The water content of the bentonite was determined for a separate sample.

2.5 Chemical composition

The chemical composition of the bulk material and of the Na-converted <0.5 μm fraction of the bentonite samples was determined by ICP emission and mass spectroscopy at a certified laboratory (ACME Analytical Laboratories, Canada), using standard techniques for silicate analysis ($LiBO_2/Li_2B_4O$ fusion followed by nitric acid digestion). For the bulk samples these analyses include major, minor and trace elements (incl. REE). The analyses of the <0.5 μm fractions had to be restricted to major oxides and some minor elements (by ICP-AES) due to lack of material. Loss on ignition (LOI) was determined as the weight loss on ignition of the sample at 1000º C.

Total carbon and sulphur were determined by evolved gas analysis (EGA) at the same laboratory by combustion of the samples in a Leco furnace, equipped with IR-detectors. Carbonate carbon was determined as CO_2 evolved on treatment of a subsample with hot 15% HCl.

2.6 XRD analyses

The mineralogical composition was determined by X-ray diffraction analysis of two different types of preparations, one type consisting of randomly oriented powders, and the other type consisting of aggregates with maximised preferred orientation of the clay minerals.

Random powders of bulk samples are needed for a general characterization of the bentonite and for quantitative evaluations. Also the distinction between di- and trioctahedral types of clay minerals by measurements of d(060) requires an X-ray diffraction profile of a randomly oriented sample. These specimens were prepared after grinding the bulk material to a grain-size <10 μm by use of an agate mortar. The powders were scanned in the 2θ interval 2–66° with a step size of 0.05º 2θ and a counting time of 5 s.

The weak *00l* intensities of clay minerals in a random powder make this type of preparation less suitable for clay mineral identifications. Therefore, the <0.5 μm fractions of the samples were X-ray scanned as oriented specimens, which give strongly enhanced basal (*00l*) reflections, and little or no evidence of the hk reflections of clay minerals. This type of preparation is used for identification of specific clay minerals and is necessary for tests of the swelling properties and identification of interstratified structures. In order to give unambiguous diffraction characteristics, the samples were saturated with magnesium by addition of $MgCl_2$ (0.5M). After removal of excess salt by centrifuge-washings, oriented aggregates were prepared of the clay slurry according to the "smear-on-glass" method and dried at room temperature. The oriented mounts were X-ray scanned with a step size of 0.06º 2θ and a counting time of 5 s in the interval 2–36° 2θ. In order to test the swelling properties, the samples were re-scanned after solvation with ethylene glycol (EG) at 60ºC for 48 hours.

A Seifert 3000 TT X-ray diffractometer with CuKα radiation and automatic divergence slit was used for the X-ray diffraction analyses.

2.7 Quantitative evaluation of the mineralogy

Mineral identifications were made by comparison of the diffractograms of the randomly oriented powders with the Siroquant v.30h database, Sietronics Pty Ltd. The subsequent mineral quantification was made by use of the Siroquant Analytical Software. The modelling is principally based on a Rietveld refinement method of least squares fit of calculated to measured XRD profiles (Rietveld 1969). The method is described in general and also used for montmorillonite in Taylor and Matulis (1994).

2.8 Storage of data

All data were delivered from the laboratories involved in Excel-files, which were transferred to specially adapted data templates for import to the SICADA database (Table 2-2).

Table 2-2. Data in the SICADA database.

Activity (analysis identity)	SICADA data import template	Data stored
Water soluble salts (WS) by ion chromatography	GE008 Water soluble salts	Variables vs. sample identity
CEC-determination of bulk samples (CECb) and of <0.5 µm fractions (CECc) by the Cu-trien method	GE001 Cation exchange capacity	Variables vs. sample identity
Exchangeable cations (EC) by exchange with NH_4 in alcoholic solution and ICP-AES analysis	GE001 Cation exchange capacity	Variables vs. sample identity
Chemical composition of bulk samples (EAb) and of <0.5 µm fractions (EAc) by ICP-AES/MS and evolved gas analysis	CH003 Chemical analysis of clay	Variables vs. sample identity
XRD of bulk samples; random powders (XRDb)	MA701 Sampling for XRD-analysis - bentonite	Intensity vs. 2θ angle (diffractograms)
XRD of <0.5 µm fractions; oriented mounts in air-dried (XRDc-AD) and ethylene glycol-solvated (XRDc-EG) states	MA701 Sampling for XRD-analysis - bentonite	Intensity vs. 2θ angle (diffractograms)
Quantitative evaluation of mineralogy by use of the Siroquant Software	MA701 Sampling for XRD-analysis - bentonite	Variables vs. sample identity

3 Results

3.1 Aqueous leachates

The electrical conductivity of the solutions suggests that the total salt content is lower in the coloured aggregates than in the samples of the bulk bentonite as delivered. Whereas the concentration of chloride is fairly uniform within the sample population, the coloured aggregates are distinguished by lower than average concentrations of sulphates and inorganic carbon (Table 3-1 and Figure 3-1). Sample ABF <1 mm of the fine matrix of the bentonite has the highest content of inorganic carbon, which is consistent with both the chemical and the XRD data indicating a high carbonate/calcite content in this sample (cf. Table 3-4 and Figure 3-8).

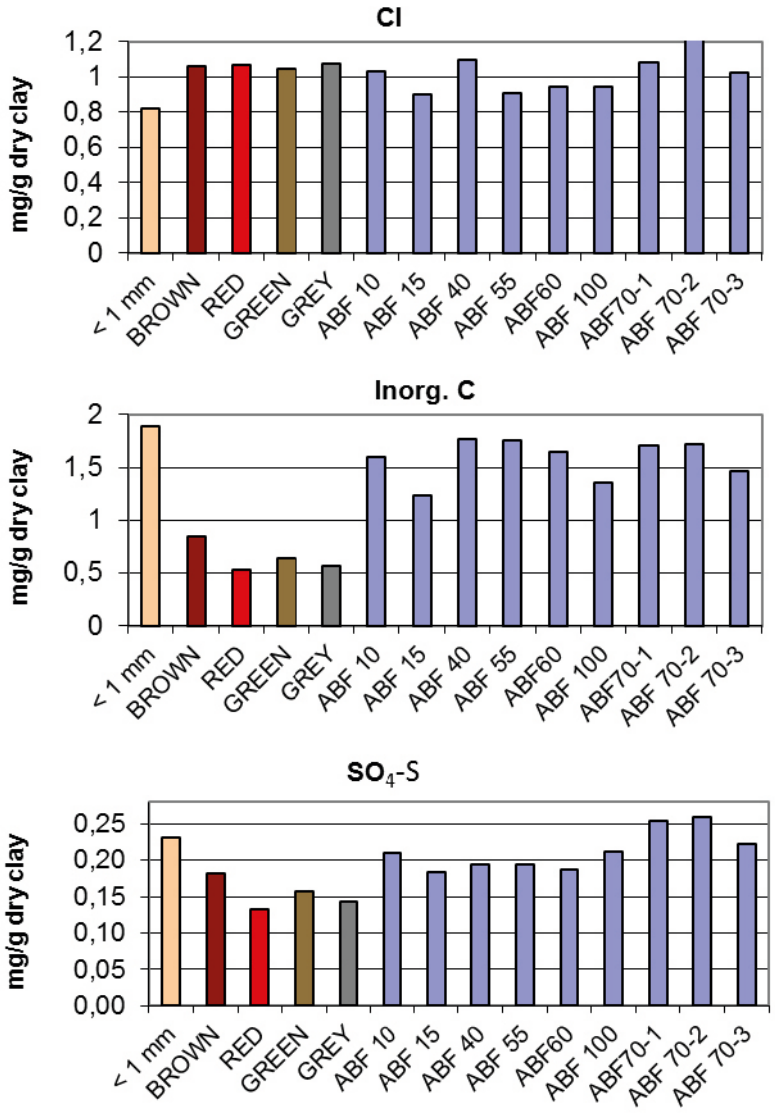

Figure 3-1. *Major anions extracted by leaching the bentonite samples with deionised water.*

Table 3-1. Major anions and inorganic carbon extracted by dispersion of bentonite in deionized water in a solid:liquid ratio 1:100.

Sample id	F	Cl	NO_3–N	PO_4–P	SO_4–S	inorg C	Kond
	mg/g dry clay						µS/cm
ABF <1 mm	0.024	0.822	0.008	0.008	0.230	1.891	262
ABF Brown	0.021	1.063	0.010	0.000	0.181	0.842	140
ABF Red	0.030	1.066	0.014	0.049	0.133	0.535	92
ABF Green	0.017	1.045	0.012	0.009	0.157	0.644	126
ABF Grey	0.021	1.078	0.018	0.000	0.142	0.563	83
ABF 10	0.018	1.031	0.012	0.000	0.209	1.597	258
ABF 15	0.014	0.904	0.010	0.008	0.184	1.238	189
ABF 40	0.031	1.093	0.006	0.000	0.194	1.773	261
ABF 55	0.015	0.905	0.011	0.005	0.194	1.760	289
ABF60	0.020	0.947	0.010	0.008	0.187	1.650	263
ABF70-1	0.030	1.083	0.005	0.000	0.254	1.708	294
ABF 70-2	0.019	1.218	0.010	0.008	0.259	1.716	296
ABF 70-3	0.019	1.022	0.008	0.000	0.222	1.460	253
ABF 100	0.015	0.946	0.009	0.000	0.212	1.356	229
Mean all (N=14)	0.021	1.016	0.010	0.007	0.197	1.338	217
St.dev	0.006	0.101	0.003	0.013	0.038	0.489	76
min	0.014	0.822	0.005	0.000	0.133	0.535	83
max	0.031	1.218	0.018	0.049	0.259	1.891	296
Mean ABF 70 (N=3)	0.023	1.108	0.008	0.003	0.245	1.628	281
St.dev	0.006	0.100	0.003	0.005	0.020	0.145	24
Mean coloured (N=4)	0.022	1.063	0.014	0.014	0.153	0.646	110
St.dev	0.005	0.014	0.003	0.023	0.021	0.139	27

3.2 Exchangeable cations and cation exchange capacity (CEC)

The data on the exchangeable cations are presented in Table 3-2 and Figure 3-2.

All samples are sodium-dominated (47–54% Na), and have calcium as the second most abundant cation (28–34% Ca). The coloured aggregates tend to have somewhat higher magnesium contents than the average of the population.

For the samples of the bulk bentonite (i.e. excl. sorted samples) the sum of cations ranges from 90 to 99 meq/100 g. This range of variation is larger than the scatter in the repeatability test performed on sample ABF 70 (range 93 to 95 meq/100 g) and also than the scatter obtained in inter-laboratory tests of the method (Dohrmann et al. 2012a).

The highest cation sums are found among the coloured samples (ABF Grey and Red), which have the highest CEC-values (cf. Table 3-3). However, the sum of cations exceeds the CEC-values in all samples (Figure 3-3) and this fact reflects the problems inherent with extraction methods for exchangeable cations: non-reactive solutes and easily soluble salts, such as chlorides and carbonates of alkali metals, will necessarily contribute to the exchangeable cation pool. For instance, approximately 3 meq cations/100 g will be derived by dissolution of chlorides according to the results of the aqueous leachates.

Table 3-2. Exchangeable cations extracted by exchange against NH_4^+ in alcoholic solution.

Sample id	Ca meq/100 g	%	K meq/100 g	%	Mg meq/100 g	%	Na meq/100 g	%	Σ cations meq/100 g
ABF <1 mm	29.9	33.7	0.7	0.8	16.5	18.6	41.6	46.9	89
ABF Brown	29.3	30.8	0.8	0.8	19.1	20.1	46.1	48.4	95
ABF Green	28.5	30.0	0.4	0.5	19.2	20.2	46.9	49.3	95
ABF Red	30.5	30.5	0.8	0.8	22.2	22.2	46.5	46.5	100
ABF Grey	31.1	29.6	0.8	0.7	24.2	23.1	48.9	46.6	105
ABF 10	30.9	32.0	0.6	0.7	18.3	19.0	46.6	48.3	96
ABF 15	25.7	27.7	0.8	0.9	16.2	17.5	49.8	53.8	93
ABF 40	30.4	32.1	0.7	0.8	18.9	20.0	44.7	47.1	95
ABF 55	28.2	31.5	0.9	1.0	17.5	19.6	43.0	48.0	90
ABF 60	31.8	32.1	0.8	0.8	19.5	19.8	46.9	47.3	99
ABF 70-1	26.8	28.8	0.7	0.8	17.1	18.4	48.4	52.1	93
ABF 70-2	26.3	28.0	0.8	0.8	17.2	18.3	49.8	52.9	94
ABF 70-3	27.1	28.6	0.8	0.8	17.1	18.1	49.8	52.5	95
ABF 70-4	27.4	28.9	0.8	0.8	17.5	18.4	49.3	51.9	95
ABF 70-5	27.1	28.5	0.8	0.8	17.3	18.3	49.8	52.4	95
ABF 100	30.9	31.1	0.8	0.8	18.9	19.0	48.9	49.2	99
Mean all (N=16)	28.8	30	0.7	0.8	18.7	19	47.8	50	96
St.dev.	2.1	1.6	0.1	0.1	2.2	1.6	2.1	2.6	3.8
Min	25.7	28	0.4	0.5	16.2	18	41.6	47	89
Max	31.8	34	0.9	1	24.2	23	49.8	54	105
Mean ABF 70	26.9	28.5	0.8	0.8	17.3	18.3	49.4	52.4	94
St.dev.	0.40	0.35	0.02	0.02	0.17	0.14	0.59	0.39	0.8
Mean coloured	30.0	30	0.7	0.7	21.9	22	47.4	47	100
St.dev.	1.3	0.5	0.2	0.2	2.5	1.5	1.3	1.6	4.9

Table 3-3. Cation exchange capacity (CEC) in meq/100 g of bulk samples (left) and of the fractions <0.5 µm (right).

Sample id	Bulk			<0.5 µm		
	CEC_1 meq/100 g	CEC_2	CEC_{mean}	CEC_1 meq/100 g	CEC_2	CEC_{mean}
ABF <1 mm	84	83	83	105	103	104
ABF Brown	87	86	87	103	102	102
ABF Grey	94	95	95	117	116	117
ABF Red	94	94	94	111	110	110
ABF Green	92	91	91	103	102	103
ABF 10	87	86	87	105	107	106
ABF 15	82	81	82	98	98	98
ABF 40	86	86	86	107	107	107
ABF 55	79	80	80	107	107	107
ABF 60	88	88	88	105	105	105
ABF 70-1	84	84	84	102	102	102
ABF 70-2	84	83	83	103	104	103
ABF 70-3	83	84	84	104	103	104
ABF 100	89	92	90	110	109	110
mean all (N=14)			87			106
st.dev.			4.6			4.6
min			80			98
max			95			117
mean ABF 70 (N=3)			84			103
st.dev.			0.4			0.9
mean coloured (N=4)			92			108
st.dev.			3.7			6.8

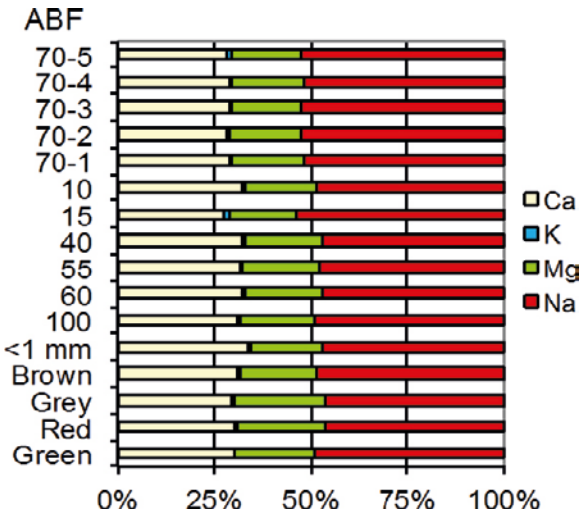

Figure 3-2. *Relative cation distribution in the sample population.*

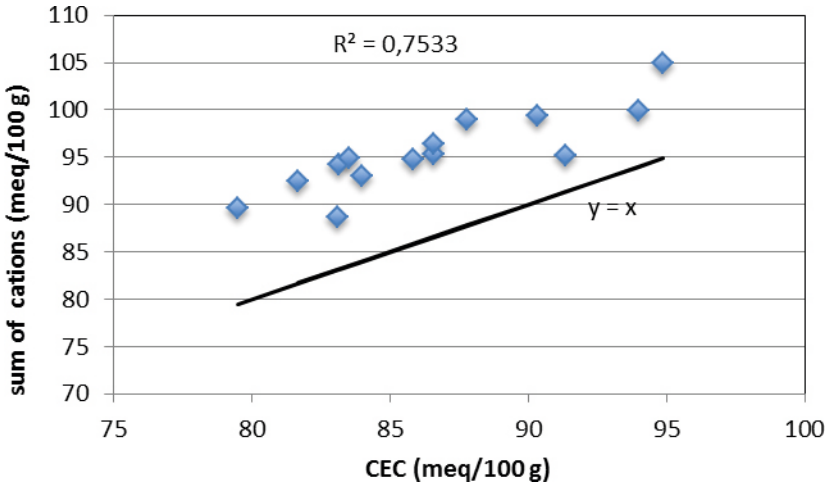

Figure 3-3. *Plot of the sum of cations against the CEC of the bulk samples.*

CEC-data and some descriptive statistical measures for the bulk samples and the <0.5 µm fractions are compiled in Table 3-3. The CEC-values of the original bulk bentonite samples (excl. sorted samples) range from 80 to 90 meq/100 g. Again, this range of variation is significantly larger than the normal scatter in the Cu-trien method, as exemplified by the repeatability test on sample ABF 70 (83–84 meq/100 g), and as demonstrated in inter-laboratory tests of the method (Dohrmann et al. 2012b). Primarily, the proportion of smectite in a bulk sample determines the CEC and according to the XRD data fairly large proportional variations exist among the samples. For instance, the samples with the lowest CEC, ABF 55 and ABF<1 mm, have the highest proportion of quartz and calcite, whereas samples with maximum CEC-values, ABF Red and Grey, are more or less devoid of other non-clay minerals than iron oxides. Iron oxides and oxyhydroxides in the Asha bentonite occur not only as discrete phases, but are also closely associated with the clay minerals, on the surfaces of which they may form "coatings", thereby modifying the properties of the clay minerals, particularly the ion exchange behavior. Cations can, for instance, be attracted to charged, hydroxylated surfaces of the iron phases if the pH of the reagent solution used in the CEC-determination is more alkaline than the pH of the zero point of charge of the iron phase.

The mean CEC of the <0.5 µm fractions is 106 meq/100 g (std. dev. 4.6). Again, samples ABF Grey and ABF Red, together with the reddish ABF 100, are distinguished by values higher than the average. However, there is no straightforward coupling between the CEC of the <0.5 µm fractions and the charge of the smectite, because all <0.5 µm fractions contain variable, although small, amounts of a fine-grained kaolin mineral, i.e. a clay mineral with low cation exchange capacity, and of iron oxyhydroxides (cf. chapter 3.6).

3.3 Chemical composition of bulk samples

The chemical compositions are listed together with some descriptive statistical measures in Table 3-4 (bulk samples) and Table 3-5 (Na-saturated <0.5 µm fractions).

Sulphide, sulphur and organic carbon are considered potentially harmful in a tunnel backfill material, but currently there are no stipulated threshold values for these substances (SKB 2010).

Carbon. The total carbon content, ranging from 0.03 to 0.96% C, is more or less equal to the acid soluble carbon content (as CO_2 in Table 3-4), which indicates that the major fraction of carbon is derived from carbonates (Figure 3-4). The data for the <0.5 µm fractions suggest, however, that minor amounts of colloidal organic matter may exist.

All coloured aggregates are very low in carbonates, whereas samples ABF <1 mm of the fine-grained matrix, together with ABF 55, has the maximum acid-soluble carbon content, corresponding to 8–9% $CaCO_3$, if all acid-soluble carbon is allocated to calcite (cf. chapter 3.5 Mineralogy). The rest of the samples have values intermediate these extremes.

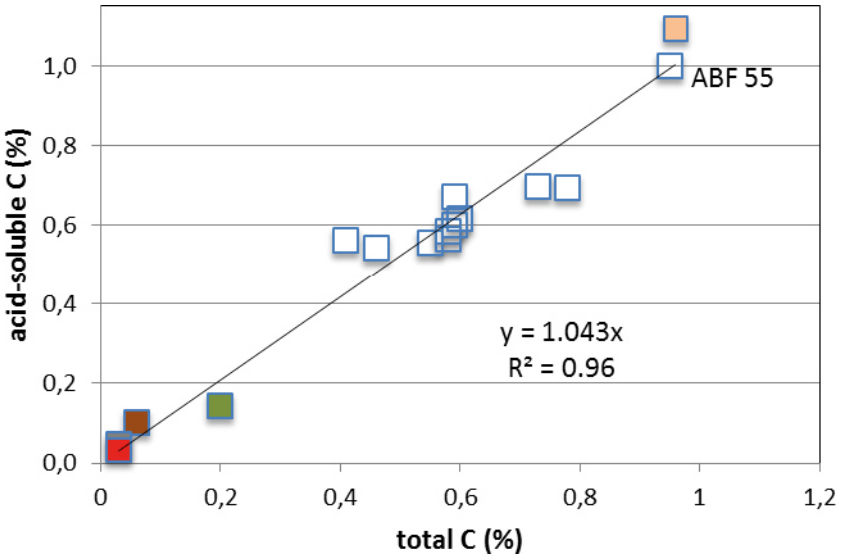

Figure 3-4. *Plot of acid-soluble carbon against total carbon. The coloured squares represent ABF Red, Grey, Brown, Green and <1 mm.*

Sulphur. The total sulphur content is close to or below the detection limit (0.02%) in all samples and, according to the results of the aqueous leachates, the major fraction of sulphur exists as sulphate (gypsum).

Major oxides. Comparisons of the major oxide composition are based on ratios of the oxides rather than percentage values, in order to avoid artefacts caused by variations in LOI, i.e. in the amount of volatiles in the samples. The ratios SiO_2/Al_2O_3 and Al_2O_3/MgO ratios (Figure 3-5) were selected to illustrate the compositional variation among the samples, which is considerably larger than the scatter in the repeatability test performed on sample 70.

The iron-rich Asha bentonite has high concentrations also of other heavy metals, but their concentrations are not uniform within the sample population. The lowest concentrations of, for instance, Mn, Cu, Co and Ni are found in ABF Red and ABF Grey, but samples ABF 100, ABF 10 and/or ABF 40 tend to cluster together with these coloured samples at the lower concentration range. In contrast, samples ABF 15 and ABF 70 are found together with the matrix sample ABF <1 mm in the upper concentration range (cf. Table 3-4).

A similar grouping pattern is indicated in the distribution of the rare earth elements, which is illustrated by the bar graphs of Figure 3-6, in which the samples were sorted in order of increasing concentration for the maximum possible number of the REEs (minor REE were excluded).

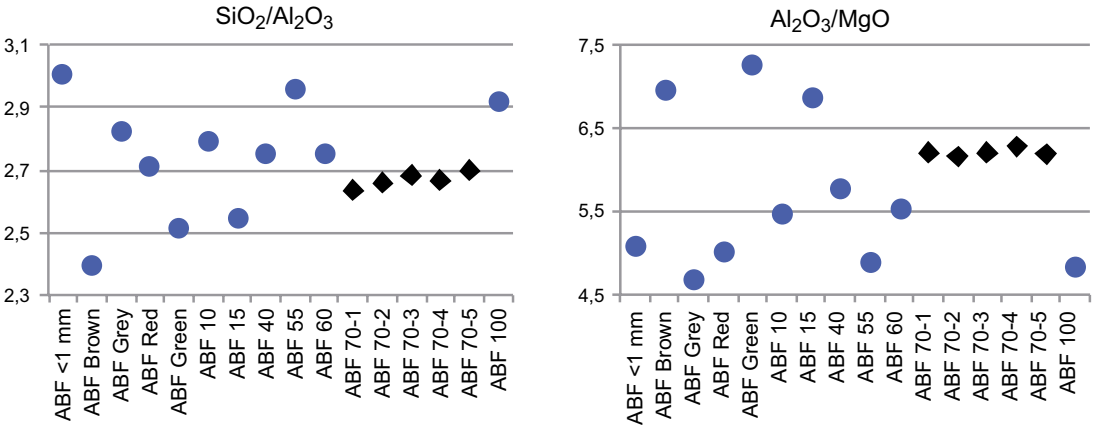

Figure 3-5. *Plot of the SiO_2/Al_2O_3 and Al_2O_3/MgO ratios of the bulk samples. Black diamonds =five subsamples of ABF 70 analysed for test of repeatability.*

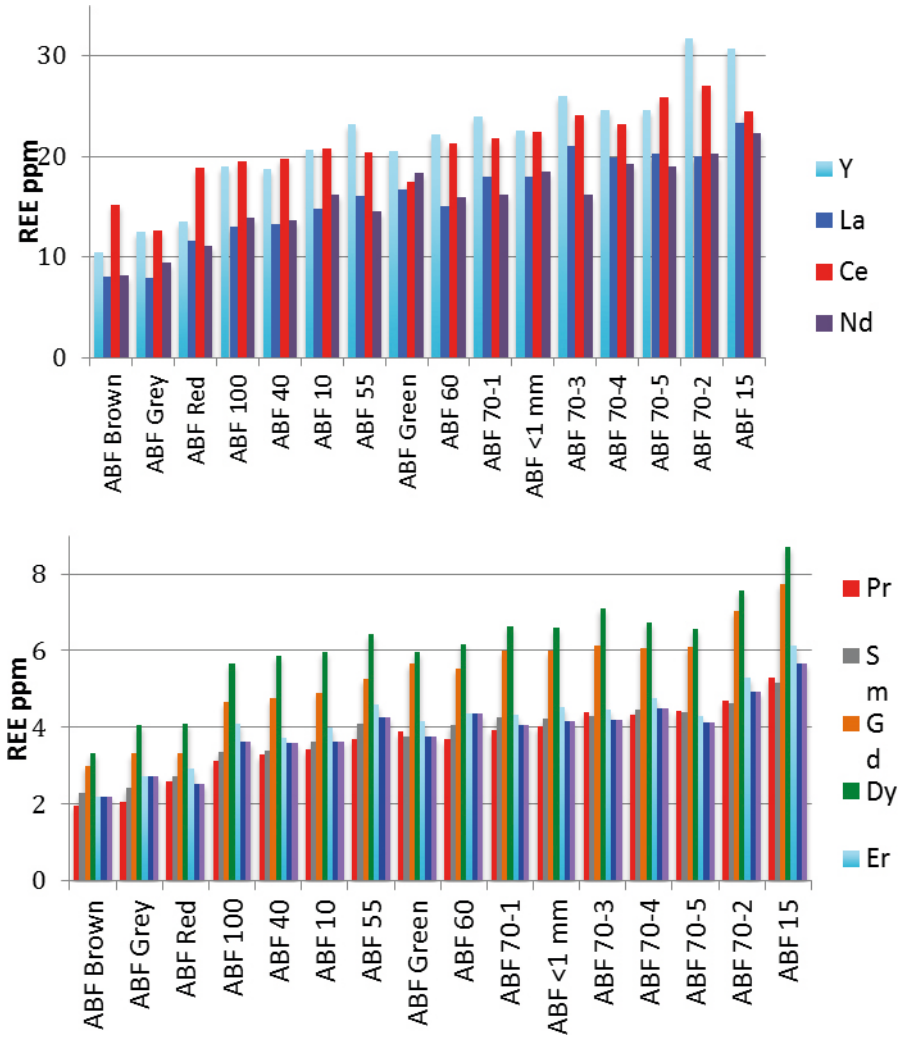

Figure 3-6. *Distribution of the major REE within the sample population. The concentration of Y=2 × plotted concentration.*

Table 3-4. Chemical composition of bulk bentonite and colour-sorted samples. Analyses by ICP-AES and MS, carbon and sulphur by evolved gas analysis.

Sample id	SiO_2 %	Al_2O_3 %	Fe_2O_3 %	MgO %	CaO %	Na_2O %	K_2O %	TiO_2 %	P_2O_5 %	MnO %	Cr_2O_3 %	LOI %	Sum %	C_{tot} %	S_{tot} %	CO_2 %	Ba mg/kg	Be mg/kg	Co mg/kg	Cs mg/kg	Ga mg/kg	Hf mg/kg	Nb mg/kg	Rb mg/kg	Sn mg/kg	Sr mg/kg	Ta mg/kg
DL	0.01	0.01	0.04	0.01	0.01	0.01	0.01	0.01	0.01	0.01	0.002	5.1	0.01	0.02	0.02	0.02	1	1	0.2	0.1	0.5	0.1	0.1	0.1	1	0.5	0.1
ABF <1 mm	42.24	14.04	11.52	2.76	6.08	1.28	0.14	0.84	0.23	0.24	0.020	20.4	99.82	0.96	<0.02	4.01	100	1	67.9	0.3	13.8	2.3	7.1	5.6	<1	304	0.4
ABF Brown	42.83	17.86	12.33	2.57	1.31	1.35	0.06	1.15	0.14	0.12	0.03	20.1	99.85	0.06	<0.02	0.37	15	<1	56.5	0.3	14.9	2.3	10.6	2.6	<1	170.6	0.6
ABF Red	44.39	16.38	12.07	3.26	1.16	1.30	0.14	0.96	0.26	0.09	0.026	19.8	99.86	0.03	<0.02	0.12	23	<1	40.1	0.2	14.2	1.8	9.3	5.8	<1	199	0.5
ABF Green	44.51	17.71	10.51	2.44	1.40	1.39	0.05	1.15	0.12	0.06	0.034	20.5	99.85	0.20	<0.02	0.53	8	<1	38.6	0.1	17.5	1.9	10.4	2.9	1	171	0.7
ABF Grey	44.92	15.93	12.29	3.41	1.14	1.36	0.12	0.93	0.22	0.08	0.027	19.4	99.87	0.03	<0.02	0.17	17	<1	43.2	<0.1	13.8	1.6	7.6	4.1	<1	207.6	0.5
ABF 10	43.36	15.55	11.89	2.84	4.21	1.38	0.09	0.97	0.23	0.15	0.025	19.1	99.84	0.73	<0.02	2.55	41	<1	54.1	0.2	16.1	2.0	8.9	4.2	<1	229.5	0.5
ABF 15	42.09	16.54	13.24	2.41	3.20	1.47	0.10	1.09	0.15	0.17	0.026	19.3	99.83	0.41	0.02	2.06	80	<1	67.1	0.3	16.7	2.6	10.2	5.1	<1	190.2	0.5
ABF 40	44.00	16.01	11.47	2.78	3.63	1.37	0.09	1.02	0.17	0.13	0.028	19.1	99.85	0.46	<0.02	1.99	39	<1	51.7	0.3	15.7	2.2	9.3	4.0	<1	210	0.6
ABF 55	42.07	14.24	11.81	2.91	6.40	1.33	0.17	0.90	0.29	0.24	0.024	19.4	99.83	0.95	0.02	3.66	77	<1	71.3	0.2	14.4	2.2	7.9	6.4	<1	252.9	0.5
ABF 60	43.69	15.89	11.86	2.88	4.19	1.38	0.10	0.99	0.20	0.14	0.026	18.5	99.83	0.78	<0.02	2.54	40	<1	60.4	0.3	15.5	1.6	9.6	4.4	<1	214.7	0.7
ABF 70-1	42.74	16.23	12.12	2.62	3.62	1.51	0.10	1.00	0.17	0.17	0.024	19.5	99.83	0.60	0.05	2.26	88	<1	69.5	0.3	15.7	1.7	9.7	5.1	<1	209.6	0.5
ABF 70-2	42.73	16.08	12.39	2.61	3.51	1.47	0.10	1.04	0.15	0.15	0.025	19.6	99.82	0.59	0.03	2.46	67	<1	70.1	0.2	15.5	1.8	10.6	5.3	<1	215.5	0.5
ABF 70-3	43.20	16.11	12.08	2.60	3.41	1.48	0.12	1.07	0.15	0.15	0.024	19.5	99.84	0.58	0.02	2.14	54	<1	57.8	0.2	14.3	2.2	10.8	5.2	<1	216.7	0.6
ABF 70-4	42.85	16.07	12.26	2.56	3.68	1.47	0.12	1.03	0.16	0.16	0.025	19.4	99.83	0.58	<0.02	2.07	57	<1	58.4	0.2	14.8	2.2	9.6	5.4	<1	206.3	0.5
ABF 70-5	42.90	15.90	12.13	2.57	3.73	1.45	0.10	1.01	0.14	0.15	0.025	19.5	99.84	0.59	<0.02	2.20	77	<1	53.9	0.2	13.9	2.0	9.4	4.9	<1	232.4	0.5
ABF 100	43.83	15.03	10.81	3.11	4.17	1.39	0.18	0.85	0.50	0.14	0.021	19.8	99.86	0.55	<0.02	2.04	49	<1	49.8	0.2	14.6	2.2	8.2	6.4	<1	209.9	0.5
all (N=16)																											
mean	43.27	15.97	11.92	2.77	3.43	1.40	0.11	1.00	0.22	0.15	0.026			0.51		1.95	52		56.9	0.2	15.1	2.0	9.3	4.8		215	0.5
stdev	0.88	1.00	0.64	0.29	1.57	0.07	0.03	0.09	0.10	0.05	0.003			0.30		1.14	28		10.6	0.1	1.1	0.3	1.1	1.1		31	0.1
min	42.07	14.04	10.51	2.41	1.14	1.28	0.05	0.84	0.12	0.06	0.02			0.03		0.12	8		38.6	<0.1	13.8	1.6	7.1	2.6		171	0.4
max	44.92	17.86	13.24	3.41	6.08	1.48	0.18	1.15	0.50	0.24	0.034			0.96		4.01	100		71.3	0.3	17.5	2.6	10.8	6.4		304	0.7
ABF 70 (N=5)																											
mean	42.88	16.08	12.20	2.59	3.59	1.48	0.10	1.03	0.21	0.16	0.02			0.59		2.23	69		61.9	0.22	14.8	2.0	10.0	5.2		216	0.5
stdev	0.19	0.12	0.13	0.03	0.13	0.02	0.01	0.03	0.11	0.01	0.00			0.01		0.15	14		7.4	0.04	0.8	0.2	0.6	0.2		10	0.0
coloured (N=4)																											
mean	44.16	16.97	11.80	2.92	1.25	1.35	0.09	1.05	0.19	0.09	0.03			0.08		0.30	16		44.6	0.2	15.1	1.9	9.5	3.9		187	0.6
stdev	0.92	0.96	0.87	0.49	0.12	0.04	0.04	0.12	0.07	0.03	0.00			0.08		0.19	6		8.2	0.1	1.7	0.3	1.4	1.5		19	0.1

Table 3-4 continued.

Sample id	Th mg/kg	U mg/kg	V mg/kg	W mg/kg	Zr mg/kg	Y mg/kg	La mg/kg	Ce mg/kg	Pr mg/kg	Nd mg/kg	Sm mg/kg	Eu mg/kg	Gd mg/kg	Tb mg/kg	Dy mg/kg	Ho mg/kg	Er mg/kg	Tm mg/kg	Yb mg/kg	Lu mg/kg	Sc mg/kg	Mo mg/kg	Cu mg/kg	Pb mg/kg	Zn mg/kg
DL	0.2	0.1	8	0.5	0.1	0.1	0.1	0.1	0.02	0.3	0.05	0.02	0.05	0.01	0.05	0.02	0.03	0.01	0.05	0.01	1	0.1	0.1	0.1	1
ABF <1 mm	1.7	0.5	217	<0.5	85.6	45.1	18.0	22.4	4.01	18.4	4.21	1.68	5.98	1.08	6.59	1.56	4.53	0.66	4.16	0.66	44	0.3	148.7	2.8	92
ABF Brown	1.7	0.4	301	<0.5	79	20.9	8.0	15.2	1.96	8.1	2.27	0.72	2.98	0.53	3.32	0.74	2.19	0.34	2.18	0.32	51	0.1	119.4	0.7	123
ABF Red	1.6	0.5	127	<0.5	63.5	27.1	11.6	18.8	2.59	11.1	2.72	0.98	3.33	0.64	4.08	0.94	2.91	0.41	2.52	0.39	50	0.2	97.2	1.9	71
ABF Green	1.6	0.3	235	<0.5	77.8	41	16.7	17.4	3.87	18.3	3.74	1.48	5.66	1	5.95	1.4	4.16	0.56	3.75	0.49	52	0.1	112.7	0.7	93
ABF Grey	1.4	0.4	146	<0.5	56.1	24.9	7.9	12.6	2.06	9.4	2.4	0.89	3.31	0.63	4.04	0.84	2.73	0.4	2.7	0.37	49	0.1	82.0	0.8	75
ABF 10	1.8	0.6	228	0.6	83.5	41.4	14.7	20.8	3.42	16.2	3.63	1.36	4.9	0.95	5.96	1.38	3.98	0.58	3.63	0.55	47	0.2	117.0	1.3	88
ABF 15	1.9	0.6	252	<0.5	91.4	61.4	23.3	24.4	5.29	22.3	5.17	1.96	7.74	1.38	8.7	2.13	6.13	0.89	5.66	0.83	50	0.2	132.7	1.6	104
ABF 40	2.1	0.4	220	<0.5	78.2	37.4	13.2	19.7	3.27	13.6	3.37	1.38	4.74	0.9	5.86	1.27	3.74	0.59	3.58	0.55	48	0.2	119.3	1.4	91
ABF 55	1.9	0.6	221	<0.5	84.5	46.3	16.0	20.4	3.7	14.5	4.08	1.5	5.26	1.01	6.42	1.46	4.6	0.68	4.25	0.71	45	0.4	144.4	2.8	97
ABF 60	1.8	0.5	216	<0.5	70.8	44.3	15.0	21.3	3.67	15.9	4.06	1.49	5.53	1.04	6.17	1.54	4.37	0.66	4.34	0.63	48	0.2	118.8	1.6	91
ABF 70-1	1.8	0.4	218	0.6	78.3	47.9	18.0	21.7	3.92	16.2	4.26	1.46	5.99	1.02	6.64	1.53	4.34	0.64	4.06	0.63	49	0.3	130.4	2.0	96
ABF 70-2	3.4	0.6	225	<0.5	85.8	63.4	20.0	27.0	4.69	20.2	4.62	1.57	7.03	1.21	7.57	2.01	5.3	0.78	4.92	0.80	48	0.3	126.6	3.3	95
ABF 70-3	1.9	0.5	215	<0.5	85.9	52	21.0	24.1	4.39	16.1	4.28	1.48	6.12	1.06	7.11	1.7	4.47	0.66	4.19	0.66	48	0.3	131.8	2.3	97
ABF 70-4	1.8	0.5	215	<0.5	83.8	49.1	19.8	23.2	4.33	19.2	4.47	1.63	6.07	1.13	6.72	1.68	4.75	0.66	4.49	0.64	48	0.3	136.8	2.0	101
ABF 70-5	3.1	0.6	217	<0.5	82.4	49.1	20.2	25.8	4.41	18.9	4.4	1.51	6.09	1.05	6.55	1.57	4.29	0.69	4.13	0.66	47	0.2	137.1	1.9	97
ABF 100	1.5	0.4	150	<0.5	67.2	38	13.0	19.5	3.11	13.9	3.36	1.28	4.65	0.89	5.67	1.32	4.09	0.61	3.61	0.59	44	0.2	111.8	2.2	76
all (N=16)																									
mean	1.9	0.5	213		78.4	43.08	16.03	20.89	3.67	15.77	3.82	1.40	5.34	0.97	6.08	1.44	4.16	0.61	3.89	0.59	48	0.2	122.9	1.8	93
stdev	0.5	0.1	42		9.5	11.78	4.50	3.77	0.92	3.90	0.82	0.31	1.32	0.22	1.35	0.38	0.96	0.14	0.88	0.14	2.3	0.09	17.14	0.76	12.32
min	1.4	0.3	127		56.1	20.9	7.9	12.6	1.96	8.1	2.27	0.72	2.98	0.53	3.32	0.74	2.19	0.34	2.18	0.32	44	0.1	82.0	0.7	71
max	3.4	0.6	301		91.4	63.4	23.3	27.0	5.29	22.3	5.17	1.96	7.74	1.38	8.7	2.13	6.13	0.89	5.66	0.83	52	0.4	148.7	3.3	123
ABF 70 (N=5)																									
mean	2.4	0.5	218		83.2	52.30	19.80	24.36	4.35	18.12	4.41	1.53	6.26	1.09	6.92	1.70	4.63	0.69	4.36	0.68	48	0.3	132.5	2.3	97
stdev	0.8	0.1	4		3.1	6.39	1.10	2.09	0.28	1.86	0.15	0.07	0.43	0.08	0.42	0.19	0.41	0.06	0.35	0.07	0.71	0.04	4.45	0.58	2.28
coloured (N=4)																									
mean	1.6	0.4	202		69.1	28.48	11.05	16.00	2.62	11.73	2.78	1.02	3.82	0.70	4.35	0.98	3.00	0.43	2.79	0.39	51	0.1	102.8	1.0	91
stdev	0.1	0.1	81		11.2	8.74	4.14	2.71	0.88	4.55	0.67	0.33	1.24	0.21	1.12	0.29	0.83	0.09	0.68	0.07	1.29	0.05	16.71	0.59	23.69

Table 3-4 continued.

Sample id	Ni mg/kg	As mg/kg	Cd mg/kg	Sb mg/kg	Bi mg/kg	Ag mg/kg	Au mg/kg	Hg mg/kg	Tl mg/kg	Se mg/kg
DL	0.1	0.5	0.1	0.1	0.1	0.1	0.5	0.01	0.1	0.5
ABF <1 mm	52.3	<0.5	0.1	<0.1	<0.1	<0.1	2.5	<0.01	<0.1	<0.5
ABF Brown	49.6	<0.5	<0.1	<0.1	<0.1	<0.1	1.3	<0.01	<0.1	<0.5
ABF Red	38.3	<0.5	0.1	<0.1	<0.1	<0.1	<0.5	<0.01	<0.1	<0.5
ABF Green	30.8	<0.5	0.3	<0.1	<0.1	<0.1	<0.5	<0.01	<0.1	<0.5
ABF Grey	41.5	0.5	<0.1	<0.1	<0.1	<0.1	<0.5	<0.01	<0.1	<0.5
ABF 10	41.3	0.6	<0.1	<0.1	<0.1	<0.1	1.5	<0.01	<0.1	<0.5
ABF 15	46.4	<0.5	<0.1	<0.1	<0.1	<0.1	2.1	<0.01	<0.1	0.5
ABF 40	39.8	<0.5	<0.1	<0.1	<0.1	<0.1	3	<0.01	<0.1	<0.5
ABF 55	60.3	0.6	0.1	<0.1	<0.1	<0.1	3.6	<0.01	<0.1	<0.5
ABF 60	43.2	<0.5	0.1	<0.1	<0.1	<0.1	1.9	<0.01	<0.1	<0.5
ABF 70-1	46.5	<0.5	0.1	<0.1	<0.1	<0.1	3.9	<0.01	<0.1	<0.5
ABF 70-2	54.8	0.6	<0.1	<0.1	<0.1	<0.1	27.1	<0.01	<0.1	<0.5
ABF 70-3	51.0	<0.5	<0.1	<0.1	<0.1	<0.1	20.1	<0.01	<0.1	<0.5
ABF 70-4	47.2	<0.5	<0.1	<0.1	<0.1	<0.1	5.1	<0.01	<0.1	<0.5
ABF 70-5	48.9	0.7	0.2	<0.1	<0.1	<0.1	6.9	<0.01	<0.1	0.5
ABF 100	43.7	<0.5	1.4	<0.1	<0.1	<0.1	1.1	<0.01	<0.1	<0.5
all (N=16)										
mean	46.0						6.2			
stdev	7.09						8.04			
min	30.8									
max	60.3									
ABF 70 (N=5)										
mean	49.7						12.6			
stdev	3.35						10.38			
coloured (N=4)										
mean	40.1									
stdev	7.79									

Table 3-5. Chemical composition of Na-saturated <0.5 µm fractions. Analyses by ICP-AES, carbon and sulphur by evolved gas analysis.

Sample id	SiO_2 %	Al_2O_3 %	Fe_2O_3 %	MgO %	CaO %	Na_2O %	K_2O %	TiO_2 %	P_2O_5 %	MnO %	Cr_2O_3 %	LOI %	Sum %	C_{tot} %	S_{tot} %	Cu mg/kg	Ba mg/kg	Zn mg/kg	Ni mg/kg	Co mg/kg	Sr mg/kg	Zr mg/kg	Ce mg/kg	Y mg/kg	Nb mg/kg	Sc mg/kg
DL	0.01	0.01	0.04	0.01	0.01	0.01	0.01	0.01	0.01	0.01	0.002	5.1	0.01	0.02	0.02	5	5	5	20	20	2	5	30	3	5	1
ABF <1 mm c	52.33	19.76	8.04	2.83	0.31	2.58	0.05	0.21	0.02	0.08	0.026	13.6	99.95	0.19	<0.02	94	17	128	72	46	8	46	34	11	<5	45
ABF Brown c	51.25	20.55	8.66	2.40	0.06	2.80	0.07	0.18	0.02	0.05	0.038	13.8	99.94	0.18	0.03	76	<5	129	68	37	3	44	<30	7	10	47
ABF Red c	52.97	19.54	7.59	3.15	0.10	2.86	0.09	0.25	0.07	0.05	0.029	13.2	99.95	0.21	<0.02	73	<5	95	52	36	4	49	<30	19	<5	52
ABF Green c	52.07	20.83	8.03	2.33	0.09	2.77	0.02	0.20	0.02	0.03	0.044	13.5	99.97	0.25	<0.02	78	<5	129	55	35	3	46	<30	9	<5	49
ABF Grey c	53.34	18.99	7.26	3.27	0.13	2.98	0.07	0.25	0.04	0.04	0.033	13.5	99.95	0.20	<0.02	75	<5	128	59	33	4	44	<30	13	5	51
ABF 10c	52.65	19.79	8.24	2.65	0.31	2.59	0.04	0.23	0.04	0.06	0.029	13.3	99.96	0.14	<0.02	80	7	114	70	38	9	45	<30	10	<5	46
ABF 15c	51.50	21.21	8.11	2.36	0.48	2.21	0.08	0.21	0.02	0.05	0.030	13.6	99.96	0.18	<0.02	81	15	126	75	43	11	54	<30	14	<5	48
ABF 40c	52.67	19.64	8.17	2.71	0.34	2.55	0.05	0.23	0.03	0.06	0.030	13.4	99.96	0.17	<0.02	82	6	124	65	35	9	47	<30	12	<5	46
ABF 55c	52.49	19.26	7.93	2.89	0.32	2.62	0.07	0.20	0.04	0.07	0.024	14.0	99.95	0.23	<0.02	83	16	119	65	45	8	45	<30	12	10	44
ABF 60c	52.12	19.92	7.87	2.72	0.34	2.61	0.07	0.22	0.03	0.06	0.028	13.9	99.96	0.12	<0.02	80	9	111	65	36	8	47	<30	11	6	46
ABF 70-1c	52.15	20.21	8.17	2.59	0.43	2.39	0.05	0.22	0.03	0.05	0.029	13.6	99.95	0.17	<0.02	80	8	120	73	39	9	52	<30	12	<5	47
ABF 70-2c	52.14	20.05	8.13	2.56	0.30	2.51	0.04	0.24	0.04	0.05	0.028	13.8	99.95	0.11	<0.02	80	7	117	63	39	8	52	<30	11	9	47
ABF 70-3c	52.26	20.40	8.19	2.56	0.26	2.60	0.05	0.23	0.04	0.05	0.029	13.2	99.94	0.18	<0.02	80	8	119	69	37	7	50	<30	11	<5	46
ABF 70-4c	51.78	20.40	8.23	2.57	0.23	2.62	0.04	0.23	0.03	0.05	0.029	13.7	99.96	0.14	<0.02	86	8	120	73	39	5	52	<30	12	<5	47
ABF 70-5c	51.88	20.26	8.15	2.52	0.25	2.57	0.03	0.23	0.02	0.05	0.028	13.9	99.94	0.21	<0.02	86	8	159	62	42	6	50	<30	11	5	47
ABF 100c	53.13	18.83	7.93	3.14	0.31	2.78	0.10	0.25	0.09	0.06	0.025	13.2	99.94	0.10	<0.02	89	10	109	64	40	6	53	<30	15	<5	45
all (N=16)																										
mean	52.30	19.98	8.04	2.70	0.27	2.63	0.06	0.22	0.04	0.05	0.030			0.17		81	9.9*	122	66	39	7	49		12		47
stdev	0.57	0.65	0.31	0.29	0.12	0.18	0.02	0.02	0.02	0.01	0.005			0.04		5.3	3.8	13	7	4	2	3		3		2
min	51.25	18.83	7.26	2.33	0.06	2.21	0.02	0.18	0.02	0.03	0.024			0.10		73	<5	95	52	33	3	44		7		44
max	53.34	21.21	8.66	3.27	0.48	2.98	0.10	0.25	0.09	0.08	0.044			0.25		94	17	159	75	46	11	54		19		52
ABF 70 (N=5)																										
mean	52.04	20.26	8.17	2.56	0.29	2.54	0.04	0.23	0.03	0.05	0.029			0.16		82	8	127	68	39	7	51		11		47
stdev	0.20	0.15	0.04	0.03	0.08	0.09	0.01	0.01	0.01	0.00	0.001			0.04		3.3	0.4	18	5	2	1.6	1		0.5		0.4
coloured (N=4)																76		120	59	35	4	46		12		50
mean	52.41	19.98	7.89	2.78	0.10	2.85	0.06	0.22	0.04	0.04	0.036			0.21		2.1		17	7	2	0.6	2		5		2
stdev	0.94	0.86	0.61	0.49	0.03	0.09	0.03	0.04	0.02	0.01	0.007			0.03												

* excl. coloured samples

3.4 Chemical composition of <0.5 mm fractions

The chemical composition of the Na-converted <0.5 µm fractions (Table 3-5) was used for calculations of the average structural formula of the smectite. The calculation was based on the structures of 2:1 layer silicates, assuming an anionic charge of –44, in addition to the following assumptions and simplifications:

Iron was assigned to the octahedral sheet and was assumed to be trivalent although no determination was made of the oxidation state. The assumption that all iron is present only in the ferric state may underestimate the octahedral charge. Another source of error is the occurrence of "free" iron oxyhydroxides in the clay, which is discussed further below.

Potassium (0.02–0.10% K_2O) in the Na-converted clay was considered non-exchangeable and was allocated to illite, the amount of which is too small for detection by use of XRD analysis. The proportion was calculated assuming the potassium content of illite to be 8.5%, which is intermediate between the extreme values reported for clay-sized illite (Newman and Brown 1987); the SiO_2 and Al_2O_3 contents were adjusted accordingly.

Any **calcium** that may exist after the dialysis of the Na-converted clay (0.06–0.48% CaO) was assigned to the pool of interlayer cations.

All **magnesium** was assigned to the octahedral sheet because the clay had been saturated with sodium and dialyzed prior to the chemical analysis. The interlayer charge would be underestimated if some of the magnesium found by chemical analysis of the fine clay is exchangeable.

All **silica** was allocated to the tetrahedral sheet of the smectite, although the XRD-data indicate that small amounts of a kaolin mineral exist in all samples. Quantitative estimations based on the diffraction profiles of oriented mounts were considered too uncertain and no correction was made but the occurrence of a kaolin mineral in the samples necessarily adds to the sources of error in the structural formulae, and is discussed further below.

The results of the calculations are compiled in Table 3-6. The charge of the smectite varies from 0.78 to 0.88 per formula unit, and this range of variation exceeds the scatter in the repeatability test performed on sample ABF 70 (0.80–0.82 p.f.u.). According to the calculated formulae, more than 50% of the charge is located in the tetrahedral sheet and, strictly, the smectite of all samples should be classified as beidellite rather than montmorillonite according to international nomenclature recommendations (e.g. Brindley and Brown 1980, Guggenheim et al. 2006). However, an impurity of kaolin, i.e. a 1:1 layer silicate with significantly lower SiO_2/Al_2O_3 ratio than montmorillonites, will result in overestimation of the tetrahedral charge and it is probably no coincidence that ABF Grey and ABF 100, the kaolin peaks of which are close to the detection limit (cf. chapter 3.6), have the lowest tetrahedral charge. Therefore, a classification of the smectite based on the available data must be considered uncertain and the identification at a species level of the members in the montmorillonite–beidellite series should be verified by independent tests to determine the charge distribution.

Fe exceeds Mg in the octahedral sheet in all samples. The total octahedral site occupancy in the formulae exceeds, however, the normal value of 4 per $O_{20}(OH)_4$ in dioctahedral smectites. Anomalous structural formulae may arise if, for instance, amorphous or surface-sorbed impurities are present in the clay or if interlayers are present in the smectite structure. In a previous investigation of Asha backfill bentonites, Olsson and Karnland (2009) found that around 20% of the total iron content of the fine clay fraction was extractable by the CBD-method (Mehra and Jackson 1960), which more or less selectively extracts amorphous and/or very fine-grained forms of iron oxides/oxyhydroxides. Therefore, it is strongly recommended that additional tests be applied (e.g. the CBD-method) in order to validate whether the allocation of all iron to the octahedral sheet of the smectite has a true structural foundation.

Hence, several sources of error may exist in the calculated formulae, but the match between the calculated CEC of the smectite and the measured CEC of the <0.5 µm is acceptable.

Table 3-6. Calculated structural formula of the smectite in the ABF samples. Calculated CEC values (in meq/100 g) are given for the smectite ([1]) together with the measured CEC-values of the <0.5 µm fractions ([2]).

	Asha BF 2010															
	<1 mm	**Brown**	**Red**	**Green**	**Grey**	**10**	**15**	**40**	**55**	**60**	**100**	**70-1**	**70-2**	**70-3**	**70-4**	**70-5**
Si	7.40	7.28	7.44	7.34	7.50	7.41	7.28	7.43	7.42	7.39	7.54	7.41	7.42	7.43	7.40	7.39
Al	0.60	0.72	0.56	0.66	0.50	0.59	0.72	0.57	0.58	0.61	0.46	0.59	0.58	0.57	0.60	0.61
Σ tet	8.0	8.0	8.0	8.0	8.0	8.0	8.0	8.0	8.0	8.0	8.0	8.0	8.0	8.0	8.0	8.0
Al okt	2.62	2.65	2.61	2.73	2.61	2.62	2.73	2.62	2.64	2.64	2.63	2.72	2.71	2.77	2.79	2.72
Ti	0.02	0.02	0.03	0.02	0.03	0.02	0.02	0.02	0.02	0.02	0.03	0.02	0.03	0.03	0.03	0.03
Fe^{3+}	0.87	0.95	0.82	0.87	0.78	0.89	0.89	0.88	0.85	0.86	0.86	0.89	0.89	0.89	0.90	0.89
Mg	0.61	0.52	0.67	0.50	0.69	0.57	0.51	0.58	0.61	0.58	0.67	0.56	0.55	0.55	0.55	0.54
Σ oct	4.12	4.13	4.12	4.11	4.10	4.10	4.14	4.10	4.11	4.11	4.19	4.20	4.18	4.24	4.27	4.18
Ca	0.048	0.009	0.015	0.014	0.020	0.048	0.075	0.053	0.049	0.053	0.048	0.067	0.047	0.041	0.036	0.039
Na	0.72	0.79	0.80	0.77	0.83	0.72	0.63	0.71	0.73	0.74	0.79	0.68	0.71	0.73	0.74	0.73
Interlayer charge	0.82	0.81	0.83	0.80	0.87	0.82	0.78	0.82	0.82	0.84	0.88	0.81	0.80	0.82	0.81	0.80
% tet. charge	73	89	67	83	58	72	93	70	70	73	52	73	72	70	74	76
molar weight	766	768	765	765	764	766	766	766	765	766	769	768	768	770	771	768
CEC calc.[1]	107	106	109	105	113	107	101	107	108	110	115	105	105	106	105	105
CEC meas.[2]	104	102	110	103	116	106	98	107	107	105	110	103	103	103	103	103

3.5 Mineralogy of bulk samples

3.5.1 Reproducibility in preparation and XRD-analysis of random powders

To test the reproducibility in the preparation and XRD-analysis of random powders, sample ABF 70 was ground in two batches. Two random powders were prepared of batch 1 (A and B batch 1 in Figure 3-7) and three of batch 2 (A, B and C batch 2 in Figure 3-7).

In the diffraction profiles the peak positions of the major accessory minerals are indicated together with the values d(001) and d(060) of the smectite. Basal spacings in the range 1.25–1.28 nm are typical of the monolayer hydrate of Na-smectites, which are stable at a relative humidity below 60–70%. Peak asymmetry towards the low angle side, as displayed in some of the samples, may arise when the interlayer cation pool is a mixture of mono- and divalent cations (cf. chapter 3.2). The value for d(060), 0.150 nm, is typical of dioctahedral smectites.

The XRD-profile of sample B batch 2 displays a peak of low intensity at 18.3° 2θ (d=0.485 nm), probably derived from gibbsite ($Al(OH)_3$), which can barely be detected in the rest of the subsamples of ABF-70. Some variation is seen also in the intensities of the strongest peaks of quartz and calcite, probably as an effect of variations in particles size and/or inhomogeneous mixing of the samples, which are factors of major importance in the diffraction of X–rays by mixed powders. The acceptable particle size depends on the composition of the material and the radiation used, but for most powders of clay, the optimal particle size should be less than 2 µm. However, in general it is necessary to accept a larger particle size rather than to use prolonged grinding, which may create amorphous surface layers and lattice distortions in minerals, resulting in reduced reflected X-ray intensity and peak broadening. Brindley and Brown (1980) report, for instance, that for ground quartz, a maximum intensity is obtained for particles in the 2–10 µm range.

The results of the quantitative evaluations of the five subsamples of ABF 70 are given in Table 3-9.

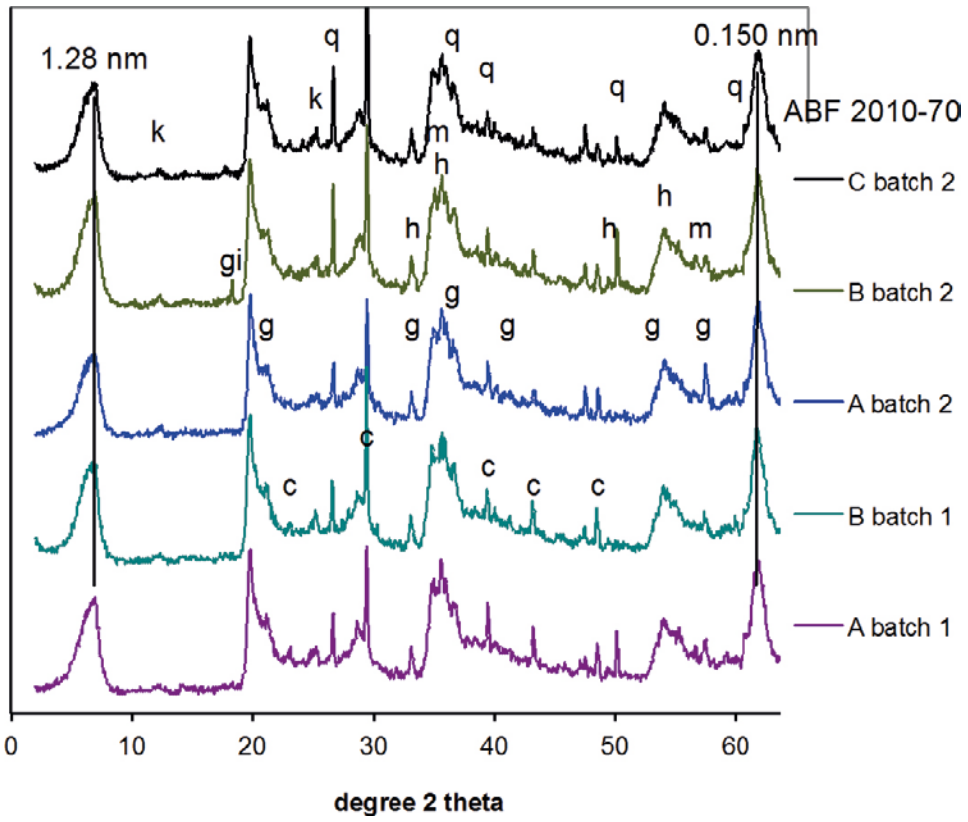

Figure 3-7. *XRD-profiles of ABF 70, ground in two batches and scanned as five random powders. The position of the strongest peaks of the major accessory minerals is indicated: c = calcite; gi = gibbsite; g = goethite; h = hematite; k = kaolin mineral; m = magnetite/maghemite; q = quartz. The d-values of the (001) and (060) smectite peaks are also indicated. CuKα radiation.*

3.5.2 Mineralogy of the coloured aggregates and matrix

Diffraction profiles of random powders of the colour-sorted aggregates and the fine-grained matrix are shown in Figure 3-8, in which the peak positions of the major accessory minerals are indicated together with the values d(001) and d(060) of the smectite.

Consistent with the chemical data, the XRD-data clearly show that calcite is concentrated in sample ABF <1 mm, consisting of the fine-grained material of the samples, whereas some of the coloured aggregates (ABF Red and Grey) are devoid of calcite. Similarly, the quantity of quartz is significant in sample ABF <1 mm, while close to or below the detection limit of the XRD-method in the rest of the samples. Hence, there are clear indications that sample ABF <1 mm has a lower smectite proportion than the rest of the samples, which is consistent with its, relatively speaking, low CEC.

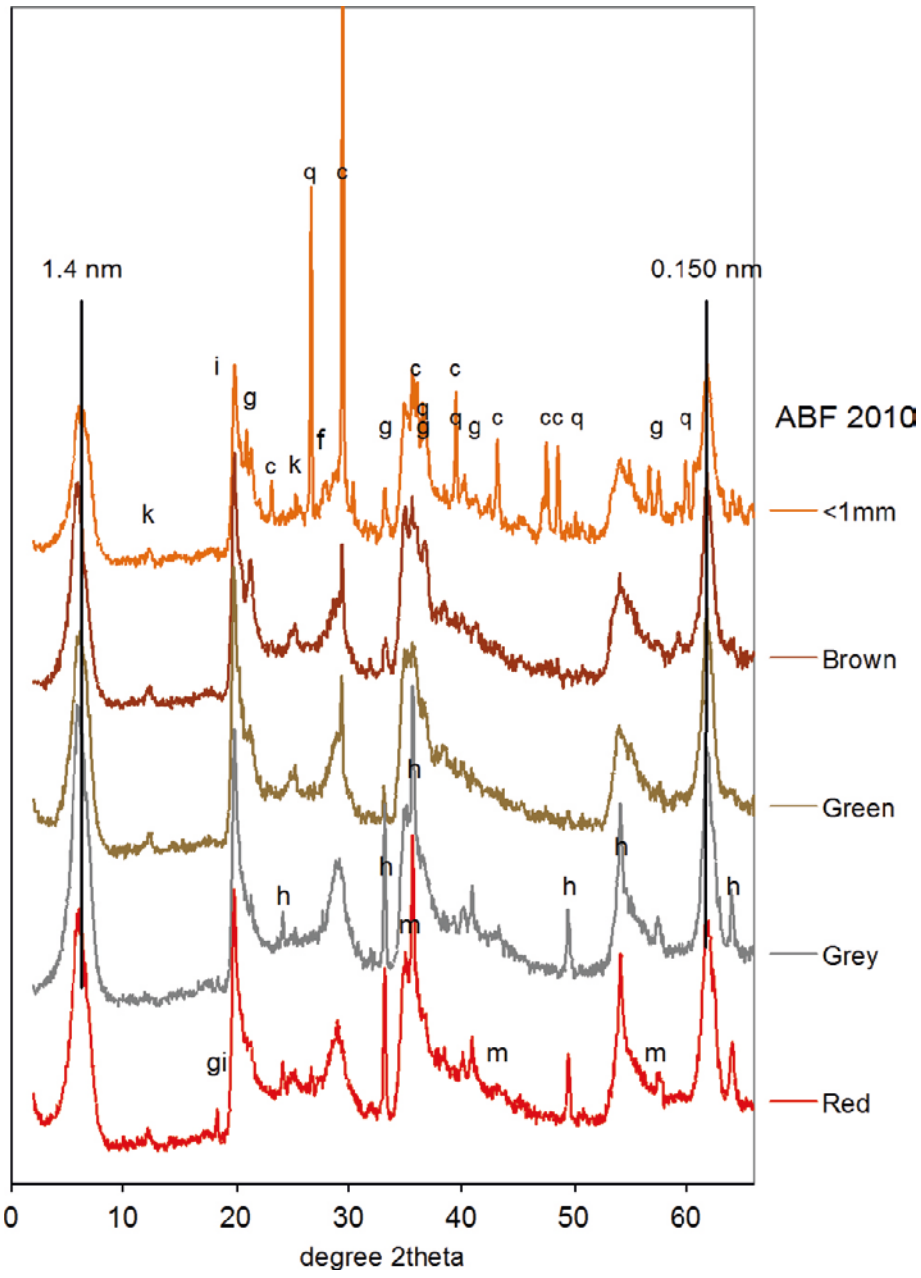

Figure 3-8. *XRD-profiles of random powders of the sorted material. The position of the strongest peaks of the major accessory minerals is indicated: c = calcite; f = feldspars; gi = gibbsite; g = goethite; h = hematite; k = kaolin mineral; m = magnetite/maghemite; q = quartz. The d-values of the (001) and the (060) smectite peaks are also indicated. CuKα radiation.*

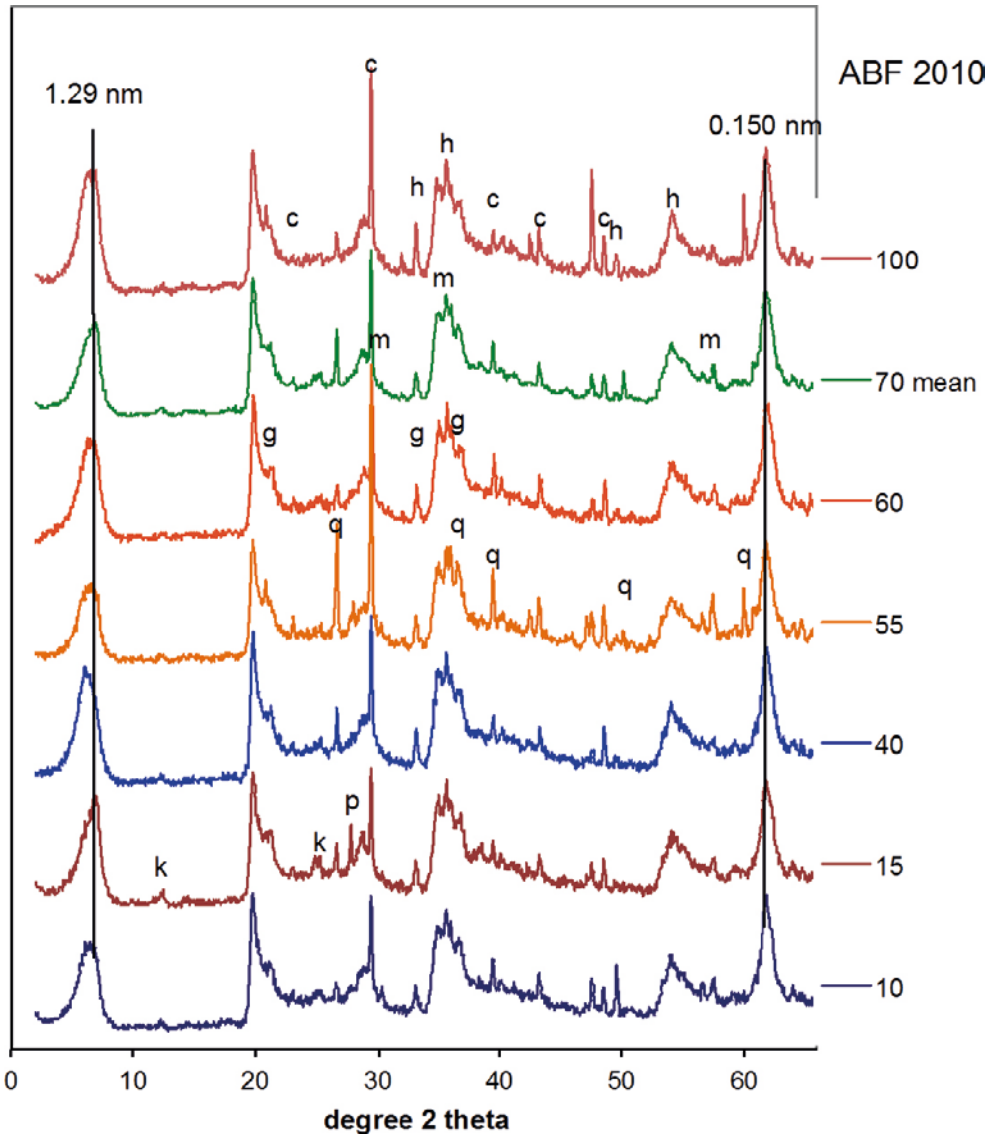

Figure 3-9. *XRD-profiles of random powders of the bulk samples of the ABF bentonite. The position of the strongest peaks of the major accessory minerals is indicated: c = calcite; g = goethite; h = hematite; k = kaolin mineral; m = magnetite/maghemite; q = quartz. The position of the (001) and the (060) smectite peaks is also indicated. CuKα radiation.*

It is also clear that the type of iron oxide minerals varies among the samples. Hematite predominates in the red and greyish red ABF Red and Grey, whereas goethite predominates in the yellowish brown samples. Also a magnetic phase, magnetite or maghemite, exists in the samples but the distinction between these minerals by XRD analysis is difficult due to the overlap of their strongest diffraction peaks. Poorly crystalline and/or very fine-grained iron oxyhydroxides are amorphous to X-rays, which implies that the iron oxyhydroxide phases may be underestimated in quantitative evaluations.

TiO_2 in the chemical analysis may exist as a discrete, crystalline phase, anatase. However, all Asha samples contain a kaolin mineral, the 002-reflection of which partly overlaps the strongest peak of anatase. The results of the quantitative evaluation are given in Table 3-7.

3.5.3 Quantitative evaluation of the bulk mineralogy

The XRD-profiles of the random powders (Figures 3-7 to 3-9) were used for a quantitative evaluation of the mineralogy by use of the Siroquant software, version 3. In the present analyses, the main minerals were identified by their typical main peaks in the XRD diffractograms, and the presence of less common minerals were checked by comparison with synthetic patterns created from the database. In this process, it is of course important not to overlook the existence of a mineral phase since this will introduce a general error equal to the content of the overlooked mineral. On the other hand, the number of possible but uncertain mineral phases should be minimized, due to the risk for accidental fit with scatter in the diffractograms, which thereby apparently reduces the content of existing phases. This also implies that phases with a calculated low content (~1%) generally should be considered uncertain. The results using the standard procedure according to the Siroquant manual are shown in Table 3-7 A. Distinction between intermediate members of the plagioclase series is complicated, and the plagioclases are therefore presented as a sum. Also maghemite/magnetite, and goethite/hematite are presented as sums.

Judged by the value of d(060) and the chemical composition, the swelling clay mineral in the Asha samples is a dioctahedral smectite of the montmorillonite–beidellite series. Montmorillonite is the dioctahedral smectite species available in the Siroquant database used for the quantitative modelling, but XRD-examination of random powders is inadequate for distinguishing the members of the series at a species-level, which motivates that the swelling clay mineral is listed as dioctahedral smectite in the tables.

Generally, it may be difficult to distinguish also between other specific clay minerals by use of Rietweld technique, especially if the clay minerals are disordered or appear as mixed layers. In the present study the proportions of smectite and kaolin are of special concern. The accuracy of the analyses was consequently checked by the following standard procedure. The total element distribution of the SQ results for each material was calculated based on the content and ideal structural formula for each identified mineral, except for smectite, for which the actual calculated structural formulas were used (Table 3-6). The calculated element distributions were compared with the results of the ICP/AES element analyses of the bulk materials (Table 3-8). A general conclusion from this comparison was that the SQ analyses overestimated i.a. the aluminum content, indicating that the kaolin content was overestimated. This indication was further supported by the ratio of the CEC of the bulk material and CEC of the <0.5 µm fraction. A second set of SQ analyses was consequently made, in which the orientation of the kaolin particles was assumed entirely random (Table 3-7 B). This increases the demands for "identification" of the kaolin mineral and in this case generally reduces the evaluated content. Repeated comparison with ICP/AES and CEC results showed significantly better concordance. For example, the mean ratio of CEC of bulk materials and CEC of <0.5 µm fractions is 0.82, which represents the mean smectite content (82% by weight) under the assumption that only smectite contributes to the CEC, and that the <0.5 µm fraction only contains smectite. This is not entirely true, but the XRD diffractograms of the <0.5 µm fraction indicate that the presence of other minerals in this size fraction is minimal. The mean content of smectite evaluated by the standard method was 75% by weight, and 84% by weight when random orientation of the kaolin mineral was assumed.

The precision of the analyses was tested by repeated sample preparations and XRD scans of sample ABF 70, followed by Siroquant analyses (Table 3-9). It is obvious that the general reproducibility is quite good, especially since some of the observed scatter may represent actual variation among the powders, as described in the previous section.

Table 3-7. Quantitative evaluation of the XRD data by use of the Siroquant software A. according to the standard procedure; B. assuming random orientation of the kaolin mineral. All figures in percentage by weight.

A	ABF 2010															
Phase	<1 mm	Brown	Grey	Red	Green	10	15	40	55	60	70 mean	100	Mean (n=12)	St. dev	Min	Max
Smectite, dioctah.	66	83	76	81	76	79	75	77	70	69	74	75	75	4,9	66	83
Plagioclase	<1	<1	3	<1	<1	<1	2	<1	<1	<1	<1	<1			<1	3
Calcite	8	<1	<1	<1	1	3	3	3	8	4	4	5			<1	8
Cristobalite	1	<1	1	<1	1	<1	<1	1	<1	1	<1	1			<1	1
Gibbsite	<1	<1	<1	1	<1	<1	<1	<1	<1	<1	0.2	<1				
Goethite/Hematite	7	6	11	9	7	6	7	7	7	8	7	8	8	1,4	6	11
Gypsum	<1	2	<1	<1	<1	1	1	1	<1	1	1	<1			<1	2
Kaolin	10	7	8	8	14	8	11	10	8	14	10	8	10	2,3	7	14
Maghemite/Magnetite	3	2	1	1	1	2	1	2	2	2	2	2	2	0,6	1	3
Quartz	5	<1	<1	<1	<1	<1	1	1	4	1	2	1			<1	5
Rutile/Anatase	<1	<1	<1	<1	<1	<1	<1	<1	<1	<1	<1	<1				

B	ABF 2010															
Phase	<1 mm	Brown	Grey	Red	Green	10	15	40	55	60	70 mean	100	Mean (n=12)	St. dev	Min	Max
Smectite, dioctah.	76	87	83	86	90	86	84	85	77	84	83	83	84	3,9	76	90
Plagioclase	<1	<1	3	<1	<1	<1	<1	<1	<1	<1	<1	<1			<1	3
Calcite	8	1	<1	<1	1	3	3	4	8	3	4	5			<1	8
Cristobalite	<1	1	1	<1	<1	<1	<1	<1	<1	<1	<1	<1			<1	1
Gibbsite	<1	<1	<1	1	<1	<1	<1	<1	<1	<1	<1	<1			<1	1
Goethite/Hematite	6	7	11	8	5	5	5	7	7	8	6	8	7	1,7	5	11
Gypsum	<1	1	<1	<1	<1	1	1	1	<1	1	<1	<1			<1	1
Kaolin	2	3	2	2	3	2	4	2	2	2	2	2	2,3	0,7	2	4
Maghemite/Magnetite	2	1	1	1	1	2	2	1	2	2	1	1	1	0,5	1	2
Quartz	5	<1	<1	<1	<1	<1	1	1	4	<1	1	1			<1	5
Rutile/Anatase	<1	<1	<1	1	<1	<1	<1	<1	<1	<1	<1	<1			<1	1

Table 3-8. Normative chemical composition of sample ABF Red based on the mineralogy evaluated by the Siroquant software. Random orientation of the kaolin mineral was assumed. All values in percentage by weight.

	Material		ABF Red						
Input SQ	Date, file, etc.		2013-01-11 \\CLAYSERV2008\Re Page 113:24:45						
	Composition Table for Oxides.								
	Phase		% by weight	SiO2	Al2O3	Fe2O3	MgO	CaO	Na2O
	Montmorillonite		86	50.12	18.51	7.18	2.99	0.13	2.72
	Albite(low)		0	0	0				0
	Anorthite		0	0.01	0.01			0	
	Calcite 1		0					0	
	Cristobalite		0.3	0.29					
	Goethite		2.1			1.9			
	Gypsum		0.3					0.11	
	Hematite		6.3			6.25			
	Kaolinite		1.8	0.84	0.72				
	Maghemite		0			0.02			
	Magnetite		1.4			1.4			
	Quartz		0	0					
	Rutile		0.6						
	Gibbsite		1.2		0.75				
	Siroquant	% by weight		51.26	19.99	16.75	2.99	0.24	2.72
Input ICP/AES	ICP/AES	% by weight		44.39	16.38	12.07	3.26	1.16	1.3
	Recalculated to 100%								
Results	SQ	ABF Red		53.90	21.02	17.61	3.14	0.25	2.86
	ICP/AES	ABF Red		55.61	20.52	15.12	4.08	1.45	1.63
		Difference		-1.71	0.50	2.49	-0.94	-1.20	1.23

Table 3-9. Quantitative evaluation of the XRD data for five subsamples of ABF 70 by use of the Siroquant software and assuming random orientation of the kaolin mineral. All figures in percentage by weight.

	ABF 2010						
Phase	**70 1A**	**70 1B**	**70 2A**	**70 2B**	**70 2C**	**Mean**	**St.dev.**
Smectite, dioctah.	84	84	83	83	82	83.2	0.8
Plagioclase	<1	<1	<1	<1	<1		
Calcite	3	4	3	4	6	4	1.2
Cristobalite	<1	<1	<1	<1	<1		
Gibbsite	<1	<1	<1	1	<1		
Goethite/Hematite	6	6	7	6	7	6.4	0.5
Gypsum	1	<1	1	<1	<1		
Kaolin	2	2	3	3	2	2.4	0.5
Maghemite/Magnetite	2	1	2	1	1	1.4	0.5
Quartz	1	1	1	2	2	1.4	0.5
Rutile/Anatase	<1	<1	1	<1	<1		

3.6 Mineralogy of <0.5 µm fractions

XRD-profiles of oriented mounts of the Mg-saturated, air-dried and EG-solvated <0.5 µm fractions of the samples are shown in Figure 3-10 and 3-11, respectively. Traces of a kaolin mineral occur in all samples. The reflections are indicated in the profiles of the EG-solvated samples in Figure 3-11, because the (002) kaolin peak is overlapped by the smectite peak in the profile of the air-dried sample. Judged by the relative peak intensities the kaolin content is lower in samples ABF Grey and ABF 100, while higher in ABF 15, than in the rest of the samples, but quantitative estimations based on the diffraction profiles of oriented mounts are uncertain.

Also traces of goethite appear in some of the samples (indicated in Figure 3-10), but apart from these two minerals, the <0.5 µm fractions appear to be pure smectite. It should, however, be emphasised that X-ray amorphous phases of iron oxyhydroxides may exist – the colour of the XRD-mounts ranges from reddish (ABF Red, ABF 100, ABF 10) to yellowish brown (ABF 15, ABF 55, ABF<1mm) which are not typical of purified smectites.

In the air-dried, Mg-saturated state, the smectite has a basal spacing of 1.47 nm (relative humidity 50±10%). No difference is seen in the expansion behaviour of the smectite, which expands to 1.69 nm upon EG-solvation in all samples, producing a complete rational series of basal reflections. The expansion behaviour is indicative of well-ordered stacking sequences with virtually no interstratification.

The XRD-profile of sample ABF 10 is distinguished by anomalous relative intensities of the basal smectite reflections. In this case the anomalous pattern is an artefact of a poor sample preparation and has been included only to exemplify some of the pitfalls in sample preparations for XRD-analysis of clays: precipitation of excessive magnesium chloride (marked by an arrow in Figure 3-11) in the clay upon drying has destroyed the preferred orientation of the clay minerals.

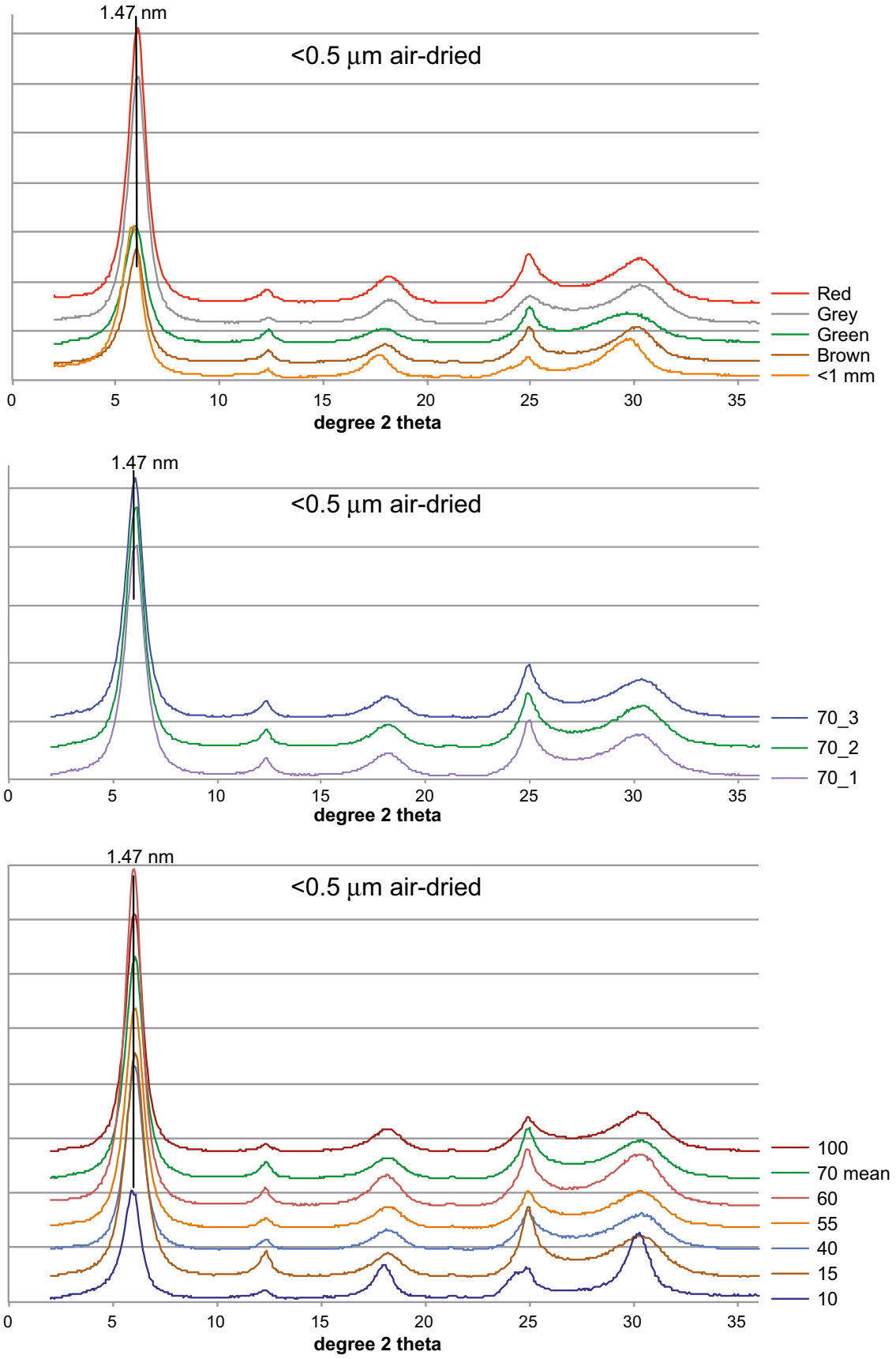

Figure 3-10. *XRD-profiles of air-dried, Mg-saturated samples of the fraction <0.5 µm. g = goethite. The position of the (001) smectite peak is indicated. CuKα radiation.*

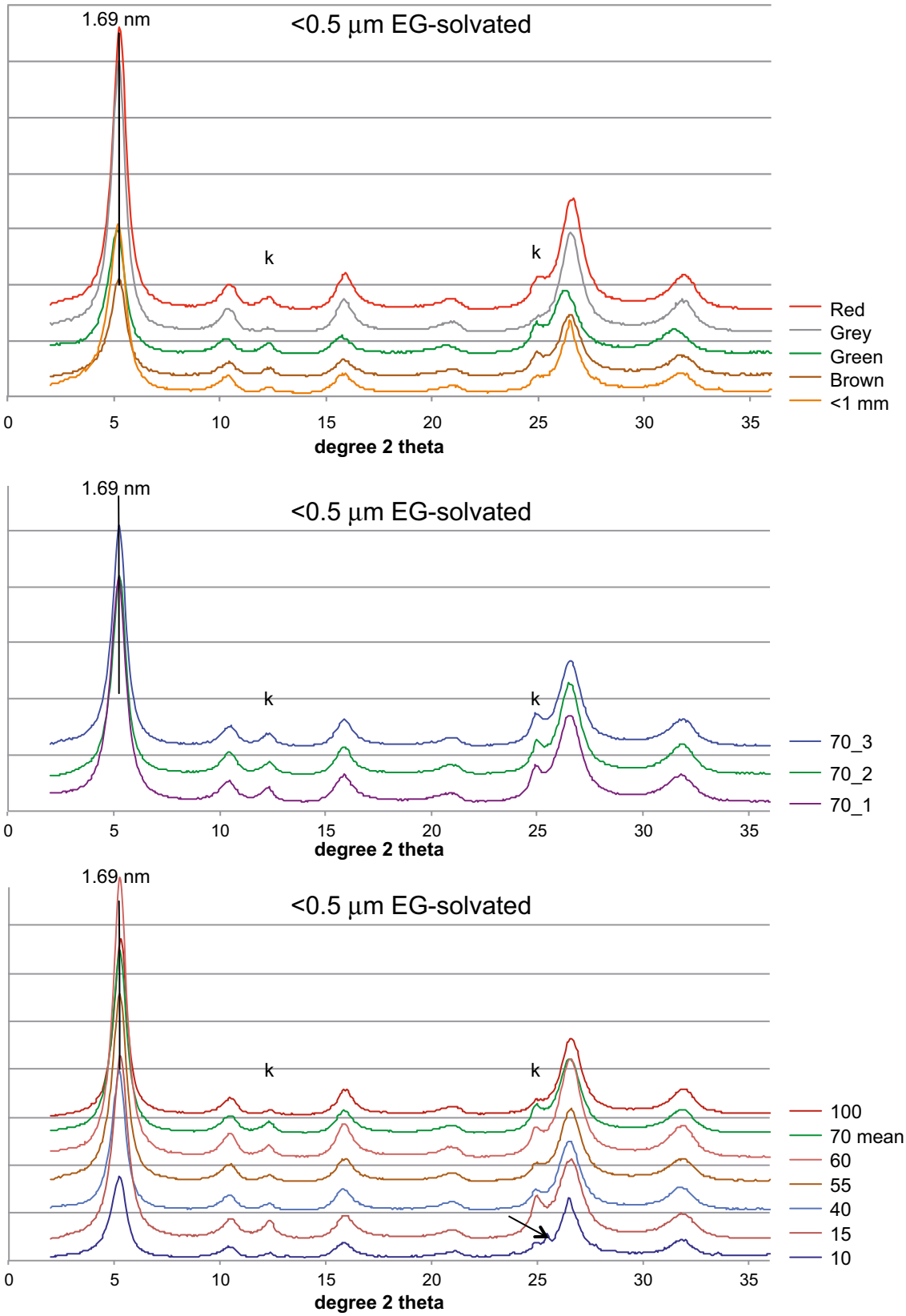

Figure 3-11. *XRD-profiles of EG-solvated, Mg-saturated samples of the fraction <0.5 µm. k = kaolin mineral. The position of the (001) smectite peak is indicated. See text for an explanation of the arrow. CuKα radiation.*

4 SKB Internal analysis – part of a knowledge transfer program

4.1 Material and methods

Samples and methods

Samples of Asha backfill bentonite (Asha NW BFL-L 2010; abbreviated Asha BF or ABF in this report) were analysed with some selected methods for chemical and mineralogical characterization (Table 4-1). The bentonite was as described earlier in this report delivered from Ashapura Minechem co. in 1250 kg sacks. The bentonites from these sacks were sampled by staff at the Äspö laboratory into 250 ml polyethene bottles.

Seven samples of the bulk materials were labelled with the number of the bottles (Table 4-1) and were ground with an agate mortel (<2 µm) for analyses of cation exchange capacity (CEC) and powder X-ray diffraction (XRD). As described earlier in this report variation of the hardness among the bentonite aggregates was noticed. Due to this hardness and lack of suitable grinding equipment some of the aggregates had to be removed when grinding the samples. The samples had thereby not been entirely homogenized, which contribute to the variations of the results. No further studies of the different particle-size bentonite aggregate of the bulk material were performed.

Sample pre-treatment

Eleven samples of the bulk material were analysed for CEC and three samples of the <0.5 µm fractions were analysed for chemical composition. Two of the three <0.5 µm fractions were exchanged to the sodium form followed by dialysis prior to chemical analysis (Table 4-1).

Table 4-1. Samples and analyses performed.

Bulk Sample id	CEC	Chemical comp.	XRD	Clay fraction (<0.5 µm) Chemical comp.
Asha BF 2010-5	2	1	1	1*
Asha BF 2010-10	2	1	1	
Asha BF 2010-15	2	1	1	
Asha BF 2010-20	2	1	1	1
Asha BF 2010-25	2	1	1	
Asha BF 2010-30	3×2	1	1	
Asha BF 2010-35	3×2	1	1	
Asha BF 2010-40	3×2	1	1	1
Asha BF 2010-45	3×2	1	1	
Asha BF 2010-50	3×2	1	1	
Asha BF 2010-55	3×2	1		
Asha BF 2010-60		1		
Asha BF 2010-65		1		
Asha BF 2010-70		1		
Asha BF 2010-75		1		
Asha BF 2010-80		1		
Asha BF 2010-85		1		
Asha BF 2010-90		1		
Asha BF 2010-95		1		
Asha BF 2010-100		1		

*Sample not Na-saturated

In order to facilitate separation of the <0.5 µm fraction, the bentonite was first suspended in deionised water and the smectite was made ion exchanged to the homoionic sodium form by washing with NaCl (p.a.;1 M), followed by centrifugation and decantation of the clear supernatant. The procedure was repeated twice. Excess salt was thereafter removed by repeated washings. The slurry was then dispersed in deionized water and centrifuged with a centrifugation time/speed calculated by use of Stokes´Law to correspond to a particle separation at an equivalent diameter of 0.5 µm. After separation the fine clay fraction was dried at 60ºC followed by dialysis (Spectra/Por® dialysis membrane 6–8000 MWCO) against deionised water until the electrical conductivity of the external water remained < 1mS/m for at least a week. The slurry was then dried at 60ºC.

Cation exchange capacity (CEC)

The CEC was determined for the bulk materials using the Cu(II)triethylenetetramine method according to Meier and Kahr (1999) with some modifications. For preparation of the Cu(II) -triethylenetetramine solution with 10 mol% excess of tri, $CuSO_4 \cdot 5H_2O$ (1.123 g, 4.5 mmol) was used.

A ground clay sample (300 ± 5 mg) was dispersed in deionised water (45 ml) followed by addition of the Cu-complex (5 ml; 45 mM Cu(II)-triethylenetetramine solution), and left on a vibrating table for 30 minutes. After centrifugation the supernatant was analysed using a spectrophotometer (Shimadzu UVPC2401 610 nm, 1 cm quarts cuvette) to determine the concentration of the Cu-complex using a calibration curve. The procedure was repeated i.e. double extractions and spectrophotometer measurements were performed and a total substitution was calculated for every sample. All CEC determinations were duplicated.

The CEC was calculated as the sum of the Cu-ions absorbed from the solutions in relation to the clay dry mass (a separate sample was taken to get the water content, drying at 105°C for 24 h). The CEC is expressed as cmol(+)/kg which is a factor of 100 times larger compared to eq/kg. The determinations were performed at three occasions (Table 4-2).

Chemical composition

The chemical composition of the bulk material and of the < 0.5 µm fractions of the bentonite samples were determined by ICP-AES/MS at ALS Scandinavia, using EPA-methods ($LiBO_2$ fusion followed by nitric acid digestion). These analyses include major oxides and some minor elements.

Due to laboratory failure of handling incoming samples, the bulk materials were not dried at 105°C. The < 0.5 µm fractions were on the other hand dried at 105°C and Loss on ignition (LOI) was determined as the difference in weight of the dried (at 105°C) and the ignited sample (at 1000°C). Total carbon, carbonate carbon and sulphur were not determined.

Powder X-ray diffraction (XRD)

Bulk clay was ground in an agate mortar, and sample holders were back loaded with the clay samples. An even surface was achieved with as little force as was possible. The diffractometer used was a Panalytical XPert Powder using a Co-tube for X-rays. The samples were scanned between 2 and 80 º2θ for approximately 90 minutes per sample. A programmable divergence slit was used together with a 20 mm mask and a 2º anti-scatter slit. A nickel filter was used to minimize the Co Kβ radiation as no monochromator was used to maximize the intensity of the X-ray beam. Two samples were heat treated at 550 ºC for one hour to confirm the validity of the identification of the kaolin mineral by turning it to amorphous metakaolin, and to give some input to the question discussed in 3.5 regarding the potential presence of anatase hidden by the kaolin reflections, that would become more visible after the removal of the kaolin mineral. The Winprep software (2006-01-17, Kenny Ståhl, DTU, Denmark) was used for background removal and minor smoothing (smoothing factor 3) of the raw data.

Storage of data

All data were delivered from the laboratories involved in Excel-files, which were transferred to specially adapted data import templates for delivery to the SICADA database.

4.2 Results

Cation exchange capacity (CEC)

The data of the cation exchange capacities are presented in Table 4-2. For the bulk bentonite samples CEC ranges from 91 to 110 cmol(+)/kg (st.dev. 5.9). A rather large difference can be seen in some cases between occasions as well as between double samples. This may indicate lack of homogenisation of the main sample (non representative samples) or lack in laboratory experience. The CEC values (Table 4-2) are generally approximately 10 cmol(+)/kg or approximately 10% higher compared to corresponding values in Table 3-3. This may be due to differences in sample pretreatment, difference in the CEC measurement or difference in the measurement of the water content. One difference between the results in Table 3-3 and Table 4-2 is that in the later two extractions were performed compared to one. The contribution of the second extraction in the SKB analysis was not insignificant, however as the procedures are not identical, it is not certain that a second extraction also would contribute in a similar way also in the Clay tech samples. Of importance is possibly also the fact that the two laboratories used different copper salts (anhydrous and salt with crystal water, respectively) in the preparation of the reagent solution. Not so many samples were common among the ones analysed, however among the clays investigated in both laboratories ABF 10 and 40 were significantly higher in CEC compared to ABF 15 and 55. More work is needed to minimize the scatter of the results and to remove the difference between the laboratories.

Chemical composition of bulk samples

The chemical compositions are listed together with some descriptive statistical measures in Table 4-3 (bulk samples) and Table 4-4 (<0.5 µm fractions). The external laboratory missed to pre-dry the sample at 105 ºC hence causing some uncertainties, however the LOI was approximately 10% compared to approximately 20% in Table 3-4. The determined chemical composition was however comparable and rather similar. Some samples being extreme in Fe such as ABF 15 were identified at both labs as an extreme, as well as high Ca in ABF 55.

Powder X-ray diffraction (XRD)

A variation in the smectite basal spacing was observed. This is caused by differences in the amount of interlayer water. The cause of this difference in water may be differences in cation population (Table 3-2) or differences in the amount of drying of the samples. The 001 basal reflection in the ABF 10 sample has its maximum towards higher angles in SKB data (Figure 5.1), while it has more of a lower angle maximum in Figure 3-9, while in both the ABF 15 samples the 001 reflection leans towards higher angles. Hence there seems to be some minor differences between the samples or their preparation. A kaolin mineral was clearly seen in all samples (Figure 4.1 and 4.2) and this kaolin reflection also disappeared upon heating (Figure 4.3; 550 ºC, 1h) which was expected (Moore and Reynolds 1997, p 234). Minor traces of what could be anatase and rutile was seen (Figure 5.3). The difference in the various samples regarding the amount of accessory minerals such as quartz, cristobalite, calcite and hematite was obvious. No significant difference could be seen in the position of the smectite 060 reflection at approximately 1.5 Å, indicating a dioctahedral smectite.

Table 4-2. Cation exchange capacity (CEC) in cmol(+)/kg of bulk samples.

Sample id	Bulk 2011-02-16 I	2011-02-16 II	2011-02-21 I	2011-02-21 II	2011-03-03 I	2011-03-03 II	2011-03-24 I	2011-03-24 II	CEC-average
Asha BF 2010- 5	101	101							101
Asha BF 2010-10	101	100							101
Asha BF 2010-15	93	93							93
Asha BF 2010-20	92	94							93
Asha BF 2010-25	97	94							96
Asha BF 2010-30			93	94	92	96	92	90	93
Asha BF 2010-35			85	101	94	94	87	86	91
Asha BF 2010-40			97	101	112	115	96	98	103
Asha BF 2010-45			115	116	112	111	100	103	110
Asha BF 2010-50			93	98	99	98	84	85	93
Asha BF 2010-55			95	90	103	96	83	85	92
Mean all (N=11)									97
St.dev.									5,9
Min									91
Max									110

Table 4-3. Chemical composition of bulk bentonite. Analyses by ICP-AES and MS.

Analyte	SiO_2	AL_2O_3	Fe_2O_3	MgO	CaO	Na_2O	K_2O	TiO_2	P_2O_5	MnO	LOI 1000°C	Sum	Ba	Be	Co	Nb	Sr	V	W	Zr	Y	Sc	Mo	Ni	Cr
Unit	%	%	%	%	%	%	%	%	%	%	%	%	mg/kg	mg/kg	mg/kg	mg/kg	mg/kg	mg/kg	mg/kg	mg/kg	mg/kg	mg/kg	mg/kg	mg/kg	mg/kg
LOQ	0.08	0.04	0.1	0.02	0.08	0.05	0.09	0.002	0.009	0.003			2	0.5	5	6	1	2	60	2	2	1	6	10	10
Sample id																									
Asha BF 2010- 5	45.6	17.4	9.75	2.82	1.18	1.38	0.0778	0.986	0.111	0.0600	8.3	87.66	3.33	0.938	47.7	10.2	165	202	<60	70.8	43.5	48.4	<6	86.0	239
Asha BF 2010-10	43.7	15.4	11.7	3.17	2.70	1.33	0.144	0.987	0.182	0.148	8.9	88.36	35.2	0.742	61.8	6.59	193	209	<60	68.7	30.7	45.7	<6	80.6	191
Asha BF 2010-15	43.1	17.6	12.7	2.42	1.23	1.50	0.0775	1.20	0.143	0.0666	8.5	88.54	<2	0.831	41.7	<6	139	241	<60	81.4	37.2	49.1	<6	75.6	182
Asha BF 2010- 20	42.5	18.0	12.1	2.32	1.29	1.32	0.0725	1.18	0.0855	0.0840	9.0	87.95	10.7	0.703	44.4	<6	144	239	<60	82.4	60.4	49.9	<6	64.0	230
Asha BF 2010-25	43.1	15.0	12.0	2.85	3.36	1.32	0.134	0.989	0.219	0.116	9.3	88.39	25.8	0.818	67.0	<6	185	207	<60	75.9	52.4	44.2	<6	93.6	170
Asha BF 2010-30	42.8	18.1	11.5	2.23	1.65	1.41	0.0663	1.19	0.0707	0.0786	9.1	88.20	13.6	0.864	34.1	<6	152	240	<60	85.1	43.3	47.8	<6	78.0	216
Asha BF 2010-35	42.0	15.0	11.5	2.93	4.56	1.27	0.145	0.937	0.275	0.140	10.2	88.96	72.7	0.872	55.2	<6	191	202	<60	82.1	43.7	45.0	<6	73.7	170
Asha BF 2010-40	43.7	15.6	11.8	2.94	3.33	1.33	0.0921	1.01	0.189	0.127	9.2	89.32	44.7	0.952	40.3	<6	199	215	<60	70.1	37.5	44.4	<6	74.8	190
Asha BF 2010-45	43.4	15.2	11.2	3.07	2.52	1.75	0.106	0.931	0.206	0.0672	8.4	86.85	13.3	0.891	42.0	8.05	151	182	<60	66.2	28.3	47.1	<6	74.4	188
Asha BF 2010-50	41.3	16.6	12.4	2.40	3.46	1.32	0.142	1.10	0.181	0.148	9.9	88.95	30.9	0.941	52.3	8.48	164	239	<60	85.8	69.5	49.5	<6	80.8	191
Asha BF 2010-55	42.4	14.3	11.6	2.87	5.84	1.30	0.192	0.887	0.300	0.204	10.7	90.59	58.1	0.943	67.5	7.69	222	215	<60	70.2	42.9	44.2	<6	81.3	163
Asha BF 2010-60	44.6	17.1	10.6	2.80	2.52	1.39	0.135	1.12	0.172	0.0777	9.1	89.61	11.4	0.785	41.7	9.95	176	240	<60	82.8	29.0	50.5	<6	70.8	218
Asha BF 2010-65	42.1	14.6	11.3	2.84	5.79	1.32	0.16	0.955	0.175	0.146	10.8	90.19	48.1	0.975	52.9	6.95	222	220	<60	83.1	36.1	45.7	<6	84.8	161
Asha BF 2010-70	42.8	18.0	12.1	2.45	1.61	1.37	0.117	1.26	0.388	0.0924	8.9	89.09	46.5	1.12	37.8	<6	155	299	<60	93.2	30.0	50.7	<6	73.9	207
Asha BF 2010-75	42.9	14.8	12.3	2.85	4.65	1.26	0.124	0.981	0.238	0.190	10.2	90.49	50.2	0.816	59.7	<6	223	238	<60	74.9	45.3	44.9	<6	86.4	160
Asha BF 2010-80	45.5	15.6	11.0	3.54	1.55	1.29	0.239	0.959	0.377	0.0773	7.8	87.93	42.8	0.800	35.6	<6	211	162	<60	63.7	37.5	45.9	<6	64.0	188
Asha BF 2010-85	39.1	16.5	11.3	2.26	5.78	1.21	0.0814	1.07	0.207	0.0870	11.8	89.40	6.96	0.721	38.9	<6	158	217	<60	73.6	43.3	47.4	<6	67.1	209
Asha BF 2010-90	43.2	15.6	11.1	2.96	3.20	1.36	0.130	1.04	0.230	0.108	9.3	88.23	20.0	0.831	47.8	7.62	179	214	<60	75.8	61.9	48.1	<6	69.6	182
Asha BF 2010-95	43.0	15.6	11.3	2.80	3.32	1.31	0.0965	1.02	0.214	0.112	9.5	88.27	16.2	0.891	38.5	<6	177	208	<60	71.2	44.6	43.7	<6	76.4	186
Asha BF 2010-100	44.6	15.1	10.5	3.40	1.99	1.39	0.217	0.885	0.420	0.0858	7.9	86.49	39.0	0.724	33.3	7.81	179	128	<60	64.2	29.3	43.4	<6	60.0	164
Mean (N=20)	43.1	16.1	11.5	2.80	3.08	1.36	0.127	1.03	0.219	0.111			31.0	0.858	47.0		179.3	215.9		76.1	42.3	46.8		75.8	190.3
Stdev	1.45	1.24	0.71	0.36	1.56	0.11	0.048	0.11	0.09	0.04			19.59	0.103	10.69		26.4	34.5		8.09	11.50	2.38		8.51	23.18
Min	39.1	14.3	9.75	2.23	1.18	1.21	0.0663	0.885	0.0707	0.0600			<2	0.703	33.3		139	128		63.7	28.3	43.4		60.0	160
max	45.6	18.1	12.7	3.54	5.84	1.75	0.239	1.26	0.420	0.204			72.7	1.12	67.5		223	299		93.2	69.5	50.7		93.6	239

Table 4-4. Chemical composition of <0.5 µm fractions. Analyses by ICP-AES and MS.

Analyte	SiO_2	AL_2O_3	Fe_2O_3	MgO	CaO	Na_2O	K_2O	TiO_2	P_2O_5	MnO	Sum	TS	LOI 1000°C	Ba	Be	Co	Nb	Sr	V
Unit	%TS	%TS	%TS	%TS	%TS	%TS	%TS	%TS	%TS	%TS	%TS	%	%TS	mg/kgTS	mg/kgTS	mg/kgTS	mg/kgTS	mg/kgTS	mg/kgTS
LOQ	0.08	0.04	0.1	0.02	0.08	0.05	0.09	0.002	0.009	0.003				2	0.5	5	5	1	2
Sample id																			
Asha BF 2010- 5*	62.4	23.9	8.51	2.97	1.05	1.33	0.103	0.151	0.0118	0.0374	100.5	90.2	9.1	8.12	0.786	27.1	<5	175	132
Asha BF 2010- 20	58.3	25.0	8.66	2.4	0.477	2.5	0.126	0.233	0.021	0.0356	97.8	91.3	8.3	8.84	1.27	28.8	<5	12.9	129
Asha BF 2010-40	59.3	23.0	8.65	2.65	0.232	2.89	<0.09	0.198	0.0184	0.0377	97.0	90.5	7.6	5.5	1.06	25.2	<5	5.95	130
mean (N=3)	60.0	24.0	8.61	2.67	0.586	2.24		0.194	0.0171	0.0369				7.49	1.039	27.0		64.6	130
std.ev.	2.14	1.41	0.084	0.286	0.4198	0.812		0.0411	0.00474	0.00114				1.758	0.2427	1.80		95.66	1.5
Min	58.3	23.0	8.51	2.4	0.232	1.33		0.151	0.0118	0.0356				5.5	0.786	25.2		5.95	129
Max	62.4	25.0	8.66	2.97	1.05	2.89		0.233	0.021	0.0377				8.84	1.27	28.8		175	132

Table 4-4 continued.

Analyte	W	Zr	Y	Sc	Mo	Ni	Cr
Unit	mg/kgTS	mg/kgTS	mg/kgTS	mg/kgTS	mg/kgTS	mg/kgTS	mg/kgTS
LOQ	0.4/0.3	2	2	1	5	10	10
Sample id							
Asha BF 2010- 5*	<0.4	47.7	7.19	40.1	<5	70.0	228
Asha BF 2010- 20	<0.4	56.9	13.7	46.5	<5	77.8	231
Asha BF 2010-40	<0.3	47.7	9.61	45.7	<5	78.1	273
mean (N=3)		50.8	10.17	44.1		75.3	244
std.ev.		5.31	3.29	3.49		4.59	25.2
Min		47.7	7.19	40.1		70.0	228
Max		56.9	13.7	46.5		78.1	273

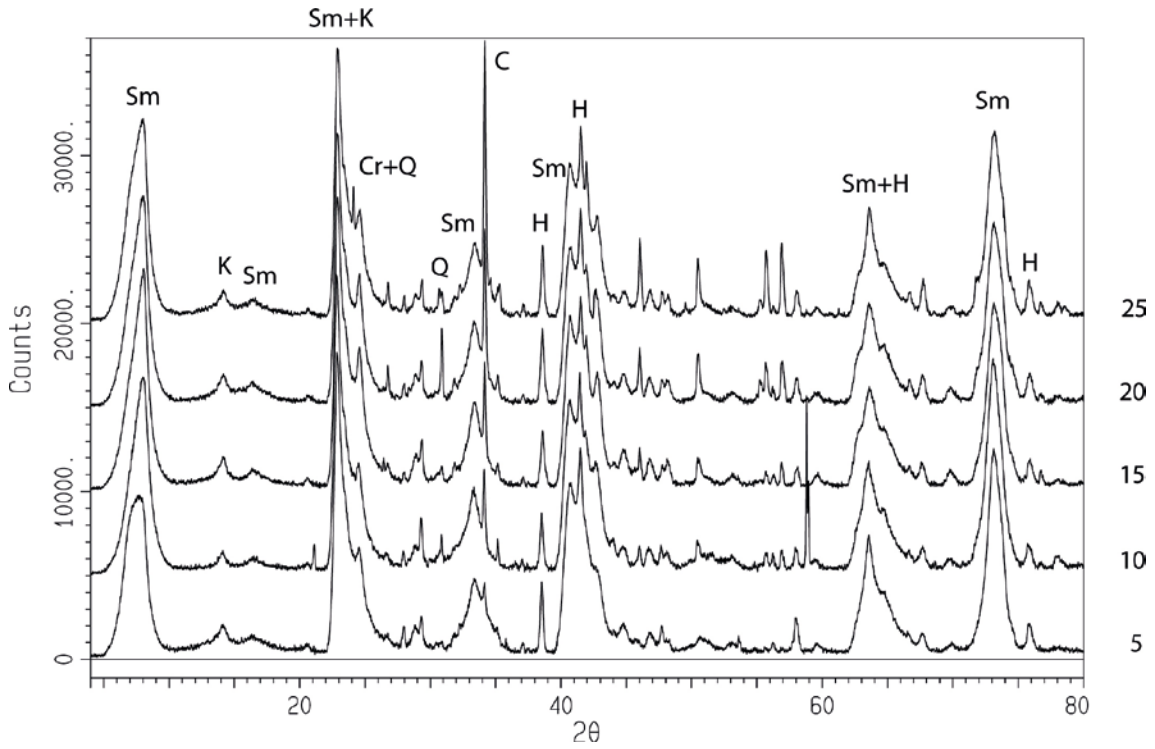

Figure 4.1. *XRD-profiles of random powders of the bulk samples 5, 10, 15, 20 and 25 of the ABF bentonite. Main minerals: Sm = smectite, K = kaolin, Cr = cristobalite, Q = quartz, C = calcite, H = hematite. CoKα radiation (λ=1.7902 Å).*

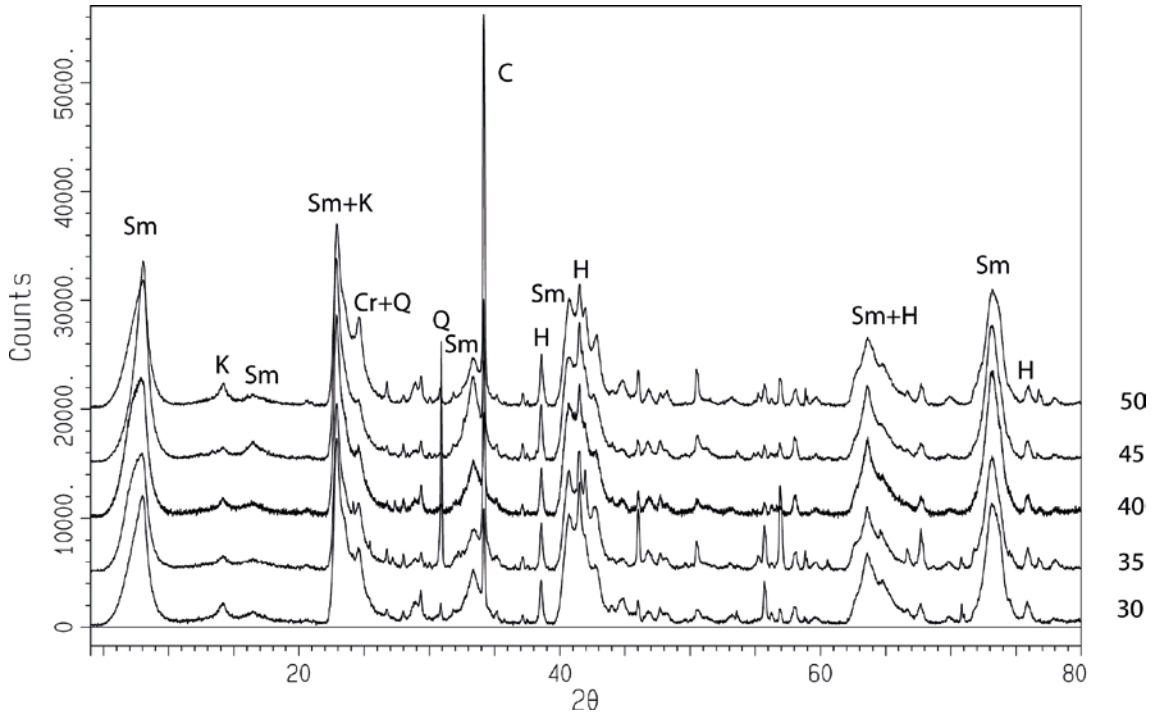

Figure 4.2. *XRD-profiles of random powders of the bulk samples 30, 35, 40, 45 and 50 of the ABF bentonite. Main minerals: Sm = smectite, K = kaolin, Cr = cristobalite, Q = quartz, C = calcite, H = hematite. CoKα radiation (λ=1.7902 Å).*

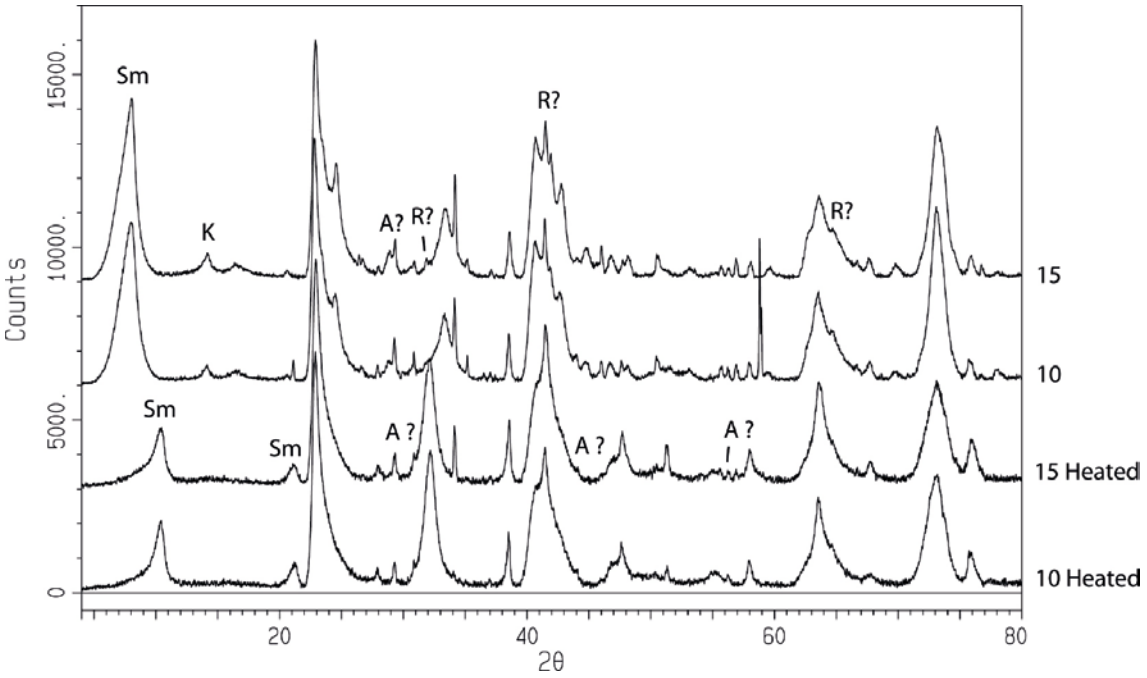

Figure 4.3. *XRD-profiles of random powders of the bulk samples 10 and 15: Before and after heat treatment at 550ºC during 1h. Notice the disappearance of the kaolin mineral. Possible traces of anatase (A) and rutile (R) are marked. CoKα radiation (λ=1.7902 Å).*

5 Conclusions

In the received state the ABF 2010 bentonite was a rather inhomogeneous material, as indicated already by large variations in the grain-size distribution and colour of the laboratory samples. As for all inhomogeneous materials, one of the most difficult aspects of establishing a specific material parameter is to obtain a small, representative sample for laboratory tests. In order to assess uncertainties related to material inhomogeneity, separate analyses were performed of aggregates >2 mm sorted by colour and of particles <1 mm from some randomly selected laboratory samples. In general, the coarse aggregates had higher smectite proportion than the fine-grained matrix of the bentonite and the overall mineralogy differed with respect to abundance and type of accessory minerals. Accordingly, a potential exists for sampling errors yielding laboratory samples of poor representativeness, if particles are segregated by size during handling and sampling of the 1250 kg sacks with bentonite. In order to reduce these errors a sampling plan designed for inhomogeneous materials should be applied.

Sulphide, sulphur and organic carbon in a tunnel backfill material are considered potentially harmful, but no threshold values have been stipulated for these substances in SKB's requirements on a tunnel backfill material. The total sulphur content of the bentonite samples from the Asha 2010 batch was close to or below the detection limit (0.02% S) of the analytical method and the major source of sulphur was sulphates.

The total carbon content of the samples ranged from 0.41 to 0.95% C, and the predominant carbon source was calcite, although the carbon data for the purified <0.5 μm fractions suggested that minor amounts of colloidal organic matter may exist.

The reference backfill material is bentonite clay with a montmorillonite content between 50 and 60% by weight, with an accepted variation within 45–90% (SKB 2010). According to the producer, Ashapura Minechem Co., the bentonite Asha NW BFL-L 2010 has a montmorillonite content of 69%. A summary of representative data of the analyzed Asha material is seen in Table 5-1.

Table 5-1. A summary of representative parameters for the Asha BF 2010 clay. The quantitative mineralogy is based on non-random orientation of the clay minerals in the XRD experiments.

Mineral phase	Weight %		Source
Smectite	75*		Table 3-7
Kaolin	10*		
Goethite/hematite	8		
Maghemite/magnetite	2		
CEC	87		Table 3-3
Element			
SiO_2	43		Table 3-4
Al_2O_3	16		
Fe_2O_3	12		
MgO	2.8		
CaO	3.4		
Na_2O	1.4		
TiO_2	1.0		
S-total	0		
C-total	0.5		
Exchangeable cations	**meq/100 g**	**Percentage of cation sum**	**Source**
Na	48	50%	Table 3-2
Mg	19	19%	
Ca	29	30%	
K	0.7	0.8%	

Based on the standard Siroquant analyses performed, the average smectite content of the ABF 2010 samples (excl. sorted samples) was 74% and the range of variation was 69 to 79%. Judged by the X-ray diffraction characteristics, the swelling clay mineral is a dioctahedral smectite of the montmorillonite–beidellite series, but the available XRD-data are inadequate for distinguishing the members of the series at a species-level. The structural formulae calculated on the chemistry of purified <0.5 μm fractions suggested that more than 50% of the charge is located in the tetrahedral sheet and, according to international nomenclature recommendations, the smectite should be classified as beidellite rather than montmorillonite. However, remnant impurities in the <0.5 μm fractions may result in overestimation of the tetrahedral charge, and the identification of the members in the montmorillonite–beidellite series at a species level should be verified by independent tests to determine the charge distribution.

A 7 Å reflection in the XRD diffractograms was interpreted as a kaolin mineral. This interpretation was confirmed by scans of heated samples, where the 7Å-phase had turned amorphous. This response of the heating distinguishes kaolin minerals from a chlorite mineral.

Most of the previous work on bentonite by SKB has been done on Wyoming MX-80 bentonite. The <0.5 μm fraction of the Wyoming bentonite is totally dominated by montmorillonite, hence the cation exchange capacity and the elemental composition of the montmorillonite are determinable by analyses of this clay fraction. The Asha backfill clay analyzed is more complex and the bulk material consisted of a substantial amount of kaolin mineral beside smectite. This complicated the Rietveld analysis, as most of the smectite and kaolin reflections in powder X-ray diffraction overlap.It also impacted on the CEC of the smectite itself, hence it was not fully reliable to estimate the total smectite content by the CEC ratio of the bentonite with the one of the smectite. The structural formula of the smectite is used to back-calculate the total chemical composition from theoretical values, to compare with the measured data. However, as the smectite structural formula was affected by the kaolin content, such calculations could not readily be done. In the Rietveld refinement, it was found that it was highly important how the orientation parameter of the kaolin was treated. The grain size of kaolin is often larger compared to the smectite minerals, however both are phyllosilicates and have a platy morphology, hence they are both very prone to orientate themselves making random orientation measurement using XRD very difficult or impossible.

To further improve the quantification of smectite in bentonites, especially with mixed clay minerals, further knowledge of the different phases present in the clay fraction is important, possibly by using alternate methods such as IR or RAMAN spectroscopy. Additionally, Rietveld analysis with XRD on prepared mixtures with known montmorillonite to kaolin ratios could be used to evaluate the correct handling of the orientation of non-smectite clay minerals.

The results in the report allow for further interpretation than has been possible within the limited time frame of the project, such as aspects concerning differences between the laboratories and the methods used. An instruction document has, however, been constructed for the CEC method. As the ABF clay has high iron content the results could also be used to evaluate differences between Co and Cu X-ray radiation in powder XRD analysis, as Cu radiation is expected to give more problematic fluorescence radiation with samples of high iron content.

Not all of the activities within the planned scope (Ch. 1) were completed but the activities were completed in order of priority. For example, the surface area measured with BET has no direct or very low impact on the performance of the backfill material. Moreover, time and cost limitations restricted the number of tests performed within this project but activities that were not carried out have been transferred to another SKB project (KBP1009) for further material knowledge and competence development.

References

SKB's (Svensk Kärnbränslehantering AB) publications can be found at www.skb.se/publications.

Ammann L, Bergaya F, Lagaly G, 2005. Determination of the cation exchange capacity of clays with copper complexes revisited. Clay Minerals 40, 441–453.

Belyayeva N I, 1967. Rapid method for the simultaneous determination of the exchange capacity and content of exchangeable cations in solonetzic soils. Soviet Soil Science, 1409–1413.

Brindley G W, Brown G (eds), 1980. Crystal structures of clay minerals and their X-ray identification. London: Mineralogical Society. (Mineralogical Society Monograph 5)

Dohrmann R, Genske D, Karnland O, Kaufhold S, Kiviranta L, Olsson S, Plötze M, Sandén T, Sellin P, Svensson D, Valter M, 2012a. Interlaboratory CEC and exchangeable cation study of bentonite buffer materials: II. Alternative methods. Clays and Clay Minerals 60, 176–185.

Dohrmann R, Genske D, Karnland O, Kaufhold S, Kiviranta L, Olsson S, Plötze M, Sandén T, Sellin P, Svensson D, Valter M, 2012b. Interlaboratory CEC and exchangeable cation study of bentonite buffer materials: I. Cu(II)-triethylenetetramine method. Clays and Clay Minerals 60, 162–175.

Guggenheim S, Adams J M, Bain D C, Bergaya F, Brigatti M F, Drits V A, Formoso M L L, Galán E, Kogure T, Stanjek H, 2006. Summary of recommendations of nomenclature committees relevant to clay mineralogy: Report of the Association Internationale pour l'Etude des Argiles (AIPEA) nomenclature committee for 2006. Clays and Clay Minerals 54, 761–772.

Mehra O P, Jackson M L, 1960. Iron oxide removal from soils and clays by a dithionite–citrate system buffered with sodium bicarbonate. In Swinwford A (ed). Clays and clay minerals: proceedings of the Seventh National conference on clays and clay minerals, Washington, DC, 20–23 October 1958. London: Pergamon Press, 317–327.

Meier L P, Kahr G, 1999. Determination of the cation exchange capacity (CEC) of clay minerals using the complexes of copper(II) ion with triethylenetetramine and tetraethylenepentamine. Clays and Clay Minerals 47, 386–388.

Moore D M, Reynolds R C, 1997. X-ray diffraction and the identification and analysis of clay minerals. 2nd ed. Oxford: Oxford University Press.

Newman A C D, Brown G, 1987. The chemical constitution of clays. In Newman A C D (ed). Chemistry of clays and clay minerals. Harlow: Longman. (Mineralogical Society Monograph 6), 2–128.

Olsson S, Karnland O, 2009. Characterisation of bentonites from Kutch, India and Milos, Greece – some candidate tunnel backfill materials? SKB R-09-53, Svensk Kärnbränslehantering AB.

Rietveld H M, 1969. A profile refinement method for nuclear and magnetic structures. Journal of Applied Crystallography 2, 65–71.

Sandén T, Olsson S, Andersson L, Dueck A, Jensen V, Hansen E, Johnsson A, 2013. Investigation of backfill candidate materials. SKB R-13-08, Svensk Kärnbränslehantering AB.

SKB, 2010. Design, production and initial state of the backfill and plug in deposition tunnels. SKB TR-10-16, Svensk Kärnbränslehantering AB.

Taylor J C, Matulis C E, 1994. A new method for Rietveld clay analysis. Part I. Use of a universal measured standard profile for Rietveld quantification of montmorillonites. Powder Diffraction 9, 119–123.